© 2018. Published by The Company of Biologists Ltd | Journal of Experimental Biology (2018) 221, jeb174458. doi:10.1242/jeb.174458

RESEARCH ARTICLE

Patterns of mitochondrial membrane remodeling parallel functional adaptations to thermal stress

Dillon J. Chung[1,*], Genevieve C. Sparagna[2], Adam J. Chicco[3] and Patricia M. Schulte[1]

ABSTRACT

The effect of temperature on mitochondrial performance is thought to be partly due to its effect on mitochondrial membranes. Numerous studies have shown that thermal acclimation and adaptation can alter the amount of inner-mitochondrial membrane (IMM), but little is known about the capacity of organisms to modulate mitochondrial membrane composition. Using northern and southern subspecies of Atlantic killifish (*Fundulus heteroclitus*) that are locally adapted to different environmental temperatures, we assessed whether thermal acclimation altered liver mitochondrial respiratory capacity or the composition and amount of IMM. We measured changes in phospholipid headgroups and headgroup-specific fatty acid (FA) remodeling, and used respirometry to assess mitochondrial respiratory capacity. Acclimation to 5°C and 33°C altered mitochondrial respiratory capacity in both subspecies. Northern *F. heteroclitus* exhibited greater mitochondrial respiratory capacity across acclimation temperatures, consistent with previously observed subspecies differences in whole-organism aerobic metabolism. Mitochondrial phospholipids were altered following thermal acclimation, and the direction of these changes was largely consistent between subspecies. These effects were primarily driven by remodeling of specific phospholipid classes and were associated with shifts in metabolic phenotypes. There were also differences in membrane composition between subspecies that were driven largely by differences in phospholipid classes. Changes in respiratory capacity between subspecies and with acclimation were largely but not completely accounted for by alterations in the amount of IMM. Taken together, these results support a role for changes in liver mitochondrial function in the ectothermic response to thermal stress during both acclimation and adaptation, and implicate lipid remodeling as a mechanism contributing to these changes.

KEY WORDS: Temperature, Acclimation, Killifish, Phospholipid, Fatty acid

INTRODUCTION

Temperature has a profound effect on the performance of ectothermic animals (Pörtner, 2001), and shapes their distribution and abundance such that the temperatures at organismal range limits are often closely correlated with their thermal tolerance limits (Sunday et al., 2011). One key way in which temperature impacts biological processes is through its effects on phospholipid membranes. As temperature increases or decreases, the fluidity of phospholipid membranes changes, which can affect the interactions and activities of enzymes embedded in the membrane environment. Thus, prolonged exposure to thermal stress is predicted to result in membrane remodeling to maintain fluidity as temperature changes; a process known as homeoviscous adaptation (HVA; Hazel, 1984; Sinensky, 1974).

Remodeling of membranes can involve alterations in the distribution of phospholipid headgroup classes [e.g. phosphatidylcholine (PC) and phosphatidylethanolamine (PE); Hazel, 1984] and their fatty acid composition. Changes in the membrane ratio of PC/PE have been associated with thermal acclimation in ectothermic species, with increases in this ratio resulting in decreased membrane fluidity (Li et al., 2006). Membrane FA composition is thought to be altered in response to thermal challenges by changing the double bond index or degree of unsaturation, with increased FA unsaturation being associated with more double bonds and greater membrane fluidity (Hazel, 1984). However, the physiological contributions of membrane remodeling through either mechanism to organismal thermal acclimation and adaptation remain poorly defined.

For most animals, aerobic metabolism is a critical process that provides the majority of the ATP needed for biological function. This ATP is generated through the action of proteins embedded in the inner mitochondrial membrane (IMM), including the proteins of the electron transport system (ETS) and the ATP synthase. The IMM is crucial, not only for the proper functioning of these proteins, but also for the maintenance of the proton-motive force used to drive ATP synthesis. Despite the importance of the IMM, relatively little is known about the extent of homeoviscous adaptation in mitochondrial membranes compared with the numerous studies of this phenomenon for the plasma membrane. Even less is known about the role of mitochondrial function and membrane properties in local adaptation to temperature, although one study identified differences in mitochondrial membrane fluidity and function among closely related species of abalone with differing geographical distributions (Dahlhoff and Somero, 1993).

There is evidence for modifications of mitochondrial membrane composition following thermal acclimation that provides some support for HVA at the level of the mitochondrion. Low-temperature acclimation has been associated with increased mitochondrial FA unsaturation in some studies (Caldwell and Vernberg, 1970; Grim et al., 2010; Itoi et al., 2003; Kraffe et al., 2007; Wodtke, 1981), but not others (Crockett et al., 2001; van den Thillart and Modderkolk, 1978). Changes in mitochondrial phospholipid class distribution in response to thermal acclimation are less clear, although effects on phospholipid FA composition may be dependent on the phospholipid class being investigated (Kraffe et al., 2007; Wodtke, 1981). Importantly, mitochondria are

[1]Department of Zoology, University of British Columbia, Vancouver, British Columbia, Canada V6T 1Z4. [2]Department of Medicine/Division of Cardiology, University of Colorado Anschutz Medical Center, Aurora, CO 80045, USA. [3]Department of Biomedical Sciences, Colorado State University, Fort Collins, CO 80523-1680, USA.

*Author for correspondence (dchungch@zoology.ubc.ca)

D.J.C., 0000-0002-0329-3828

Received 15 November 2017; Accepted 14 February 2018

Journal of Experimental Biology (2018) 221, jeb174458. doi:10.1242/jeb.174458

unique in that their membranes also contain cardiolipin (CL), a dimeric phospholipid with four FA chains that profoundly influences mitochondrial function (Chicco and Sparagna, 2007; Schlame, 2007). Cardiolipin is associated with critical mitochondrial properties, including the structural stabilization of mitochondrial electron transport complexes and the formation of mitochondrial supercomplexes (Paradies et al., 2014). In Rainbow trout, *Oncorhynchus mykiss*, high-temperature acclimation is associated with CL-specific decreases in polyunsaturated FA (PUFA) content, but the functional implications of this effect are unclear (Kraffe et al., 2007).

In contrast to the dearth of studies on mitochondrial membrane remodeling, numerous studies have detected increases in cristae surface density (and thus amount of IMM) with acclimation and adaptation to cold, although this pattern is not uniform across species (e.g. Archer and Johnston, 1991; Dhillon and Schulte, 2011). Thus, organisms have the potential to alter both the nature and the amount of IMM in response to thermal acclimation and adaptation.

In this study, we utilized the Atlantic killifish (*Fundulus heteroclitus* Linnaeus 1766) to investigate the effects of thermal acclimation and putative local adaptation on liver mitochondrial membrane remodeling and performance to assess the potential role of HVA at both physiological and evolutionary timescales. This species is found in estuarine salt marshes along a large latitudinal thermal gradient on the east coast of North America (from northern Florida, USA to Nova Scotia, Canada) and exhibits a highly eurythermal physiology (Fangue et al., 2006; critical thermal maximum, CT_{max}=34°C and CT_{min}=−1°C, for 12.5°C acclimated fish), consistent with the highly variable temperatures in its estuarine environments. In addition, this species exhibits phenotypic plasticity in response to prolonged thermal stress, recruiting a wide range of physiological mechanisms, including altered mitochondrial function (Chung and Schulte, 2015; Chung et al., 2017a,b; Fangue et al., 2009; Healy and Schulte, 2012; McBryan et al., 2016), consistent with the strong seasonal variation in habitat temperature. There are also genetically distinct northern (*Fundulus heteroclitus macrolepidotus*) and southern (*Fundulus heteroclitus heteroclitus*) subspecies of killifish that vary in their thermal tolerance limits, consistent with the latitudes at which they are found (Fangue et al., 2006). As such, this is an ideal species in which to address questions about temperature effects on mitochondrial properties with respect to both thermal acclimation and local adaptation.

In this study, we addressed the following questions: (1) Do *F. heteroclitus* subspecies differ in liver mitochondrial performance? (2) Do these subspecies alter mitochondrial performance following thermal acclimation (5, 15 and 33°C) and do these responses differ between the subspecies? (3) Is *F. heteroclitus* liver mitochondrial membrane composition and amount altered following thermal acclimation, and if so, do these changes differ between the subspecies? And (4) are variations in mitochondrial membrane composition or amount consistent with variation in mitochondrial respiratory capacity as a result of thermal acclimation and intraspecific variation? To address these questions, we employed high-resolution techniques for characterizing mitochondrial membrane composition and respiratory function between subspecies and across acclimation temperatures. Our results represent the most comprehensive investigation of these characteristics in any species to date and provide new insights into roles and potential mechanisms of mitochondrial membrane remodeling in the ectothermic response to thermal stress.

MATERIALS AND METHODS

Animals

All animal use followed University of British Columbia approved animal care protocol A11-0372. Northern (*Fundulus heteroclitus heteroclitus*) and southern (*Fundulus heteroclitus macrolepidotus*) Atlantic killifish were collected from Ogden's Pond estuary, Nova Scotia (45°71′N, 61°90′W) and Jekyll Island, Georgia (31°02′N, 81°25′W), respectively, in September 2014. Fish were transported to the UBC Aquatics Facility and housed in 190 liter recirculating tanks and were fed once daily (Tetrafin Max, Rolfe C. Hagen Inc., Montreal, QC, Canada); ambient temperature (T_a) was maintained at 15±2°C, with 20 ppt salinity, and a 12 h:12 h light:dark photoperiod. Following 10 months of holding (July 2015), fish were transferred to 114 liter tanks with T_a set at 5, 15 or 33°C, 20 ppt salinity and a 12 h:12 h light:dark photoperiod. Fish were acclimated to these conditions for 4 weeks prior to sampling.

Liver mitochondria isolation

At 09:00 h, seven killifish from an individual acclimation treatment were removed from their tank prior to daily feeding. These were the same fish used in a previous study investigating heart and brain mitochondrial function (Chung et al., 2017a). Fish were killed by severing the spine with a razor blade and were then weighed. Liver tissue was removed, weighed individually and livers from 7 individual fish were pooled and minced in ice-cold isolation buffer [250 mmol l^{-1} sucrose, 50 mmol l^{-1} KCl, 0.5 mmol l^{-1} EGTA, 25 mmol l^{-1} KH_2PO_4, 10 mmol l^{-1} HEPES, 1.5% bovine serum albumin (BSA), pH 7.4 at 20°C]. Tissue was homogenized with five passes of a loose-fitting Teflon pestle followed by filtration through one-ply cheesecloth. Crude homogenate was centrifuged at 600 ***g*** for 10 min at 4°C. The fat layer was aspirated following the slow spin and the remaining supernatant was filtered through four-ply cheesecloth. Filtered supernatant was centrifuged at 6000 ***g*** for 10 min at 4°C, followed by two washes of the resulting mitochondrial pellet. The final pellet was suspended in 800 µl of BSA-free isolation buffer and placed on ice until use in respirometry experiments. The protein content of the mitochondrial suspension was determined using a Bradford assay (Bradford, 1976) with BSA as a standard.

Mitochondrial respirometry

Mitochondrial respiratory capacity was assessed as described previously (Chung et al., 2017a) using an O2k high-resolution respirometer (Oroboros Instruments, Innsbruck, Austria). Oxygen probes were calibrated to account for background O_2 consumption and zero calibrated (using a yeast suspension) at each assay temperature (5, 15, 33 and 37°C). Two ml of assay buffer (0.5 mmol l^{-1} EGTA, 3 mmol l^{-1} $MgCl_2{\cdot}6H_2O$, 60 mmol l^{-1} lactobionic acid, 20 mmol l^{-1} taurine, 10 mmol l^{-1} KH_2PO_4, 20 mmol l^{-1} HEPES, 110 mmol l^{-1} sucrose, 1 g l^{-1} fatty-acid free BSA, pH 7.1 at 25°C) was air-equilibrated at each assay temperature followed by the addition of liver mitochondrial protein (approximately 0.5 mg). Leak respiration fueled through complex I (LEAK-I or state II) was initiated by addition of pyruvate (10 mmol l^{-1}) and malate (2 mmol l^{-1}). This was followed by an addition of ADP (2.5 mmol l^{-1}) and glutamate (10 mmol l^{-1}) yielding complex I-linked ADP-phosphorylating respiration (OXPHOS-I or state III). Succinate (10 mmol l^{-1}) was then introduced to the chamber to fuel state III respiration through complexes I and II simultaneously (OXPHOS-I+II). Carboxyatractyloside (5 µmol l^{-1}) was then introduced to the chamber to inhibit the adenine nucleotide translocator, initiating

leak respiration through complexes I and II (LEAK-I+II). Mitochondria were then fully uncoupled with repeated injections of carbonyl cyanide p-(trifluoromethoxy)phenylhydrazone (FCCP, 0.5 µmol l^{-1}) yielding substrate oxidation capacity (ETS-I+II). Complexes I, II and III were sequentially inhibited through the addition of rotenone (0.5 µmol l^{-1} in ethanol, inducing ETS-II), malonate (5 mmol l^{-1}) and antimycin A (2.5 µmol l^{-1}). Apparent respiratory capacity through cytochrome *c* oxidase (CCO) was then initiated through the addition of ascorbate (2 mmol l^{-1}) and N,N,N′, N′-tetramethyl-p-phenylenediamine (TMPD, 0.5 mmol l^{-1}). We corrected for auto-oxidation of TMPD and ascorbate via chemical background corrections at each assay temperature.

We also assessed mitochondrial OXPHOS and LEAK respiration with FA substrates, as changes in FA utilization may be associated with thermal acclimation effects on whole-organism phenotypes (Chung and Schulte, 2015). Briefly, the respirometer and mitochondria were prepared as described above. Following air calibration and the addition of the mitochondrial sample, both palmitoyl carnitine (20 µmol l^{-1}) and malate (2 mmol l^{-1}) were added to the chamber yielding LEAK-Palm. C (state II), this was followed by ADP (2.5 mmol l^{-1}) yielding OXPHOS-Palm. C (state III). All mitochondrial respiration rates were normalized to mitochondrial protein content. The remaining mitochondrial suspension was snap frozen in liquid N_2 and stored at −80°C until use for phospholipid analyses.

We estimated mitochondrial coupling with different substrates using the ratio of OXPHOS-I:LEAK-I (apparent respiratory control ratio; RCR-I); OXPHOS-I+II:LEAK-I+II (RCR-I+II) and OXPHOS-Palm. C:LEAK-Palm. C (RCR-Palm. C). We estimated the contribution of changes in total OXPHOS enzyme content to our observed thermal acclimation and subspecies effects on mitochondrial respiratory capacity by normalizing LEAK-I+II, OXPHOS-I+II and ETS-I+II to apparent CCO capacity.

Mitochondrial phospholipid extraction for PE and PC head group analysis by LC-UV detection

Phospholipids were extracted from thawed mitochondrial isolates to determine the relative proportion of membrane phosphatidylethanolamine (PE) and phosphatidylcholine (PC) and their FA compositions as previously described (Mulligan et al., 2014). This preparation results in a combined estimate of lipid composition for both the inner and outer mitochondrial membranes. Pelleted mitochondrial protein (0.5 mg) was suspended in 4 ml chloroform:methanol (2:1) with 10 mmol l^{-1} butylated hydroxytoluene (BHT) to prevent peroxidation. The solution was washed with 1 ml H_2O followed by centrifugation at 2000 ***g*** for 10 min at 4°C. Phospholipids within the chloroform phase were isolated and dried under N_2 gas and resuspended in 125 µl of hexane for analysis by normal phase HPLC (Agilent 1100 series, 50 µl injection) with an Agilent Zorbax Rx-Sil column (4.6×250 mm, 5 µm). Mobile phases of A [hexane:isopropanol:0.3 mmol l^{-1} potassium acetate (pH 7.0):acetic acid (424:566:10:0.1)] and B [hexane: isopropanol:5.0 mmol l^{-1} potassium acetate (pH 7.0):acetic acid (385:515:100:1)] were used in a gradient (flow rate=1 ml min^{-1}) from 100% A to 100% B over 6 min, mobile phase B was held for 5 min followed by a gradient back to phase A over 1 min. PE and PC were identified with a UV detector (λ=206 nm) and collected based on elution times of known standards. PE and PC content were estimated using the area under the curve of the UV signal corrected to the total area under the curve for all detected phospholipid head groups.

To determine phospholipid class-specific FA composition, PE and PC fractions were dried under N_2 gas with 7.5 µl of internal standard (heptadecanoic acid, 17:0; 0.1 mg ml^{-1}) and resuspended in 600 µl methanol. The suspension was centrifuged at 900 ***g*** for 5 min at 4°C. Sodium methoxide (25 µl, 25% stock solution) was added to the supernatant and incubated for 3 min at room temperature. The reaction was stopped with the addition of methanolic HCl (75 µl, 3 N). Fatty acid methyl esters were isolated with an addition of 700 µl hexane, followed by vortexing and centrifugation at 900 ***g*** for 1 min at 4°C. The hexane layer was isolated and dried down under N_2 gas, followed by resuspension in 50 µl of hexane for analysis using an Agilent 6890 Series Gas Chromatograph equipped with an Agilent Technologies DB-225 column (30 m×0.250 mm×0.25 µm) and flame ionization detector. Flow rate, split ratio, pressure, and velocity were set at a constant 1.7 ml min^{-1}, 1:2, 23.59 psi and 42 cm s^{-1}, respectively. Oven temperature started at 120°C, followed by an 8 min ramp at 10°C min^{-1}. This was followed by a 6 min ramp at 2.5°C min^{-1} followed by 6 min at 215°C. Individual FAs were identified based on elution time of known standards and presented as a percentage of the total phospholipid FA content.

In addition to phospholipid class-specific analyses, we characterized the FA composition of total mitochondrial phospholipids (i.e. mitochondrial membrane FA composition) frequently reported in the literature. Total mitochondrial phospholipids were extracted and immediately processed for FA analysis as described above except that 0.1 mg total protein of mitochondria was resuspended in 600 µl methanol with BHT (10 mmol l^{-1}) and 15 µl of internal standard, and a split ratio of 1:5 was used for GC analysis. FA are reported as proportions of the total phospholipid fraction. To characterize global trends in phospholipid FA characteristics potentially relevant to membrane and organismal function, we calculated ratios of monounsaturated to polyunsaturated FA (MUFA/PUFA) and n3/n6 PUFA, the double bond index (DBI; the sum of the proportions of FA multiplied by the total number of double bonds in that FA), and chain length index (the sum of the proportions of FA multiplied by the number of carbons in that FA). To evaluate potential mechanisms of altered FA distribution, we also calculated selected FA product/precursor ratios corresponding to activities of the major endogenous FA desaturation and elongation enzymes central to long-chain fatty acid biosynthesis in the liver.

Cardiolipin molecular species analysis by HPLC–ESI–MS

Given the complexity of CL composition and potential importance of specific CL molecular species (FA combinations) on mitochondrial function (Schlame, 2007), we utilized HPLC–ESI–MS to evaluate CL compositional changes as previously described (Sparagna et al., 2005). Briefly, 0.1 mg of total liver mitochondrial protein was mixed in a methanol (795 µl), chloroform (790 µl) and HCl (715 µl, 0.1 N with 11 mmol l^{-1} ammonium acetate) solution with a CL reference standard [0.081 nmol, CL with four myristoyl (14:0) FA chains]. Samples were centrifuged at 3000 ***g*** for 10 min at 4°C and the organic layer was isolated and dried under N_2 gas followed by resuspension in 100 µl of a hexane-isopropanol solution (30:40, v/v). Twenty-five µl of this phospholipid extract was injected into a normal phase HPLC column (Prodigy 5 µm silica 100 Å, 1.0×150 mm column; Phenomenex) coupled to a mass spectrometer (API 4000). Mobile phase A [hexane: isopropanol:20 mmol l^{-1} ammonium acetate in water, pH 5.5 (30:40:7)] and mobile phase B [hexane:isopropanol (30:40)] were used in a gradient (flow rate 50 µl min^{-1}) of 50% B for 6 min, increasing to 95% B over 10 min, and 95% B for 30 min followed

Journal of Experimental Biology (2018) 221, jeb174458. doi:10.1242/jeb.174458

by a return to 50% B at the end of the run. Electrospray ionization was run in negative ion mode at −4000 V, with declustering potential of −100 V, focusing potential of −350 V, and entrance potential of −10 V. Unit resolution was used with a step size of 0.1 amu over 4 s. Cardiolipin and monolysocardiolipin (containing 3 FAs; MLCL) molecular species were identified by mass/charge (m/z) ratio and quantified by comparison to the internal standard. Total CL and MLCL contents were estimated by the sum of CL and MLCL (total CL content) and MLCL species separately and normalized to the total mitochondrial MS signal. Thermal acclimation and intraspecific effects on IMM content were estimated by comparing CL content that was normalized on a per mg mitochondrial protein basis.

Data analysis

Data analysis was completed using R software (v.3.3.3). All data are means±s.e.m. with α=0.05. Sample size (n) is indicated in relevant figure or table captions. Effects of subspecies, acclimation and assay temperature on all mitochondrial respiration data were assessed using separate mixed linear models with individual set as the random effect. The effects of subspecies and acclimation temperature on mitochondrial respiratory capacity normalized to CCO capacity (assayed at 15°C) were analyzed by two-way ANOVA.

We assessed global changes in mitochondrial phospholipid head groups and fatty acids using a principal component analysis (see Table S1 for variables included in the PCA). We identified variables that contributed most heavily to each principal component by determining both the squared cosine (Cos^2) and percentage contribution factor (Ctr) of each variable within a given PC (Abdi and Williams, 2010).

A two-way ANOVA was used to assess thermal acclimation and subspecies effects on individual principal component values extracted from PC1, -2 and -3 separately. A two-way ANOVA was used to compare thermal acclimation and subspecies effects on estimates of IMM content (i.e. CL content normalized to mg mitochondrial protein).

Two-way ANOVAs with thermal acclimation and subspecies as factors were used to assess responses of whole-animal mass, liver mass, hepatosomatic index and all phospholipid (fatty acid and headgroup) data. We accounted for multiple testing in the phospholipid data by adjusting α using a Benjamini–Hochberg correction.

RESULTS

Whole organism metrics

Whole organism mass differed between subspecies ($P_{subspecies}$<0.005) and as a result of thermal acclimation (Fig. S3, $P_{acclimation}$<0.0001). The northern *F. heteroclitus* used in this study had greater whole-animal mass when compared with their southern counterparts and increasing acclimation temperature decreased whole-animal mass in both subspecies ($P_{acclimation×subspecies}$=0.195). Liver mass ($P_{subspecies}$<0.0001, $P_{acclimation}$<0.0001) and hepatosomatic index ($P_{subspecies}$<0.05, $P_{acclimation}$<0.0001) followed the same pattern as whole-organism mass, with the exception that liver mass did not differ between subspecies following acclimation to 33°C (liver mass: $P_{subspecies×acclimation}$<0.001, HSI: $P_{subspecies×acclimation}$=0.135).

Mitochondrial OXPHOS and LEAK

There were significant effects of subspecies and acclimation temperature on mitochondrial OXPHOS and LEAK respiration fueled by complex (C)I and CI+CII substrates (Fig. 1; see Table 1

Table 1. *P*-values for three-way ANOVAs of *Fundulus heteroclitus* liver mitochondrial parameters

	P-value						
Parameter	Subspecies	Acclimation temperature	Assay temperature	Subspecies×acclimation	Subspecies×assay	Acclimation×assay	Subspecies×acclimation×assay
OXPHOS-I	**<0.0005**	**<0.0001**	**<0.0001**	0.157	**<0.0001**	**<0.0001**	0.352
LEAK-I	**<0.05**	**<0.0001**	**<0.0001**	0.507	**<0.005**	**<0.0001**	0.881
OXPHOS-I+II	**<0.0005**	**<0.001**	**<0.0001**	0.413	**<0.0001**	**<0.005**	0.605
LEAK-I+II	**<0.005**	**<0.0005**	**<0.0001**	0.505	**<0.0005**	**<0.0001**	0.602
OXPHOS-Palm. C	**<0.0005**	**<0.0001**	**<0.0001**	**<0.05**	**<0.0001**	**<0.0001**	**<0.01**
LEAK-Palm. C	0.115	**<0.0001**	**<0.0001**	0.560	**<0.05**	**<0.0001**	0.811
ETS-I+II	**<0.0005**	**<0.0005**	**<0.0001**	0.406	**<0.0005**	**<0.005**	0.631
ETS-II	**<0.001**	**<0.0005**	**<0.0001**	0.419	**<0.001**	**<0.001**	0.478
CCO	**<0.01**	0.198	**<0.0001**	0.530	**<0.01**	0.344	0.975
RCR-I	0.107	0.793	**<0.0001**	0.594	0.639	0.076	0.795
RCR-I+II	0.462	0.971	**<0.0001**	0.475	0.881	0.248	0.949
RCR-Palm. C	**<0.005**	**<0.05**	**<0.0005**	**<0.05**	0.114	**<0.0005**	0.240

Significant *P*-values are in bold. OXPHOS, oxidative phosphorylation; Palm. C, palmitoyl carnitine; ETS, maximum mitochondrial substrate oxidation capacity; CCO, apparent cytochrome *c* oxidase capacity; RCR, apparent respiratory control ratio (OXPHOS/LEAK); I, flux fueled through ETS complex-I; II, flux fueled through ETS complex II; n=7–8.

Journal of Experimental Biology (2018) 221, jeb174458. doi:10.1242/jeb.174458

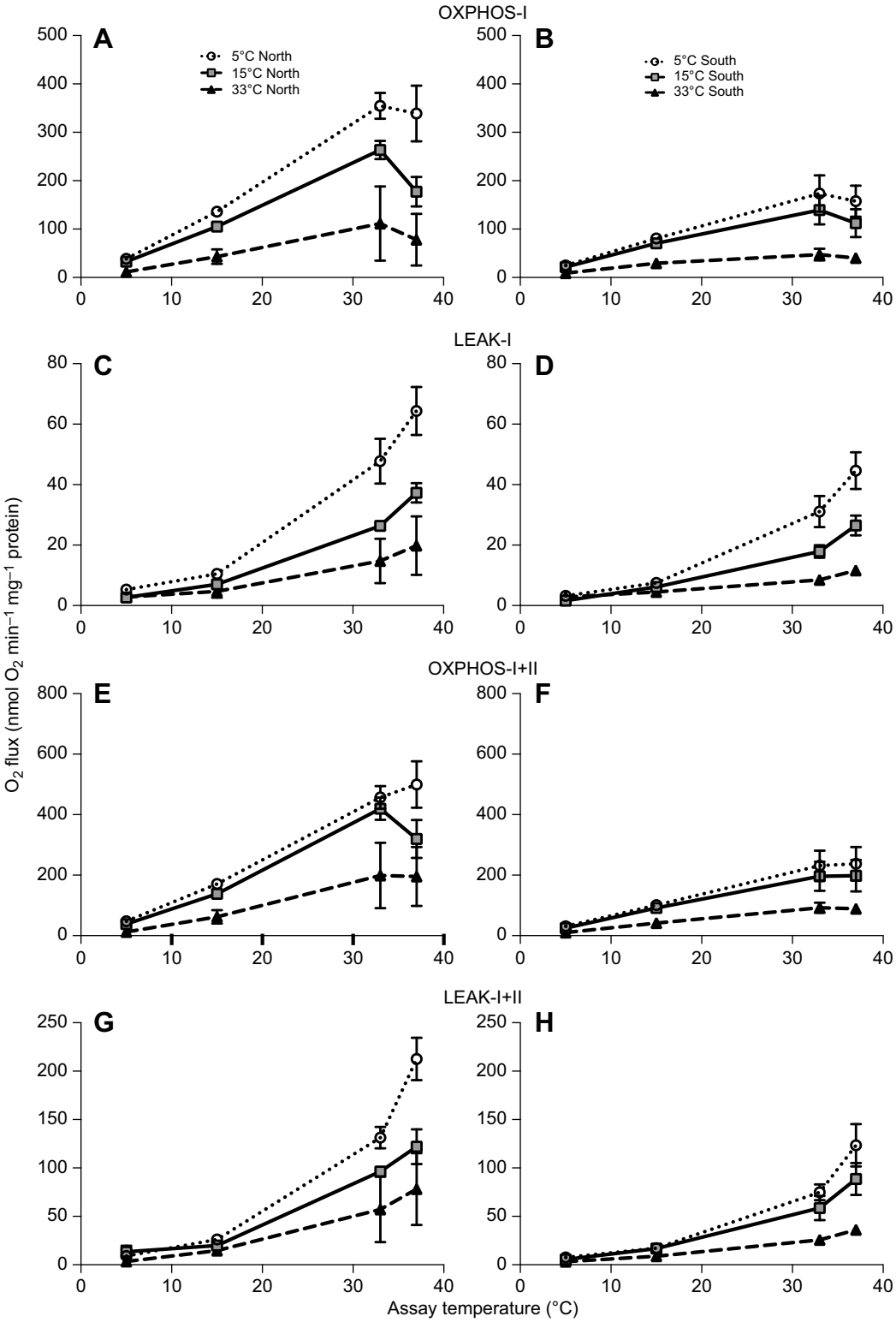

Fig. 1. Coupled mitochondrial respiration in the liver of *Fundulus heteroclitus*. Northern (A,C,E,G) and southern (B,D,F,H) *F. heteroclitus* were acclimated to 5, 15 or 33°C for 4 weeks. Oxidative phosphorylation (OXPHOS, state 3; A,B,E,F) and LEAK (C,D,G,F) respiration rate were measured through electron transport system complex I (A–D; pyruvate, malate and glutamate as substrates) and complexes I and II simultaneously (E–H; complex I substrates and succinate). Data are means±s.e.m.; see Table 1 for associated statistics (n=7–8 pooled samples, with 7 individuals per pool).

for P-values). Northern *Fundulus heteroclitus* maintained higher mitochondrial respiration rates compared with the southern subspecies at all assay temperatures. Acclimation to colder temperatures tended to increase mitochondrial OXPHOS capacity in both subspecies across assay temperatures, with no significant interaction of subspecies or acclimation effects. OXPHOS and LEAK respiration rates increased with assay temperature, although OXPHOS tended to remain similar or declined when temperature

Journal of Experimental Biology (2018) 221, jeb174458. doi:10.1242/jeb.174458

was increased from 33°C to 37°C. A greater thermal sensitivity of OXPHOS and LEAK respiration was observed in northern compared with southern *F. heteroclitus*, and in 5°C and 15°C acclimated fish when compared with 33°C acclimated fish (P<0.05 for interactions). Similar effects of subspecies, acclimation and assay temperatures were observed for OXPHOS and LEAK respiration fueled with palmitoyl carnitine (Fig. S1A-D; see Table 1 for P-values), with smaller effects of thermal acclimation and assay temperature in the southern subspecies compared with the northern subspecies (P<0.05 for three-way interaction).

Mitochondrial maximum respiratory capacity

Subspecies and thermal acclimation effects on maximum mitochondrial respiratory capacity (ETS) fueled by CI and CI+CII substrates were similar to those described for OXPHOS and LEAK respiration (Fig. 2A–D; see Table 1 for P-values), suggesting that changes in the mitochondrial content or enzymatic capacity of the ETS machinery were occurring. Apparent cytochrome *c* oxidase (CCO) capacity was higher in northern compared with southern subspecies and increased with assay temperature (Fig. 2E,F; see Table 1 for P-values). However, CCO capacity greatly exceeded the integrated ETS capacity, and was unaffected by acclimation temperature, implicating changes in upstream ETS or oxidation enzymes in the observed effects of temperature acclimation on integrated mitochondrial respiratory function in both subspecies.

Mitochondrial respiratory control

Mitochondrial respiratory control by ADP (an index of OXPHOS coupling) was evaluated by calculating OXPHOS/LEAK, known as the respiratory control ratio (RCR), for CI and CI+II substrates (Fig. 3) or FA oxidation (Fig. S1E,F; see Table 1 for P-values). We detected significant effects of assay temperature on RCR supported by CI and CI+II substrates, increasing marginally between assay temperatures of 5–15°C then decreasing beyond 15°C, but no other significant main or interaction effects were detected. However, significant interaction effects on FA-linked RCR were observed between subspecies and with thermal acclimation. In the northern subspecies, 15°C acclimated killifish exhibited greater RCR compared with ratios in fish acclimated to 5 and 33°C. In contrast, 33°C acclimated southern killifish exhibited greater FA linked RCR compared with 5 and 15°C acclimated fish. These effects were only observed at specific assay temperatures (T_{assay}=5 and 33°C in northern and southern *F. heteroclitus*, respectively), which drove a significant interaction between assay temperature and thermal acclimation effects.

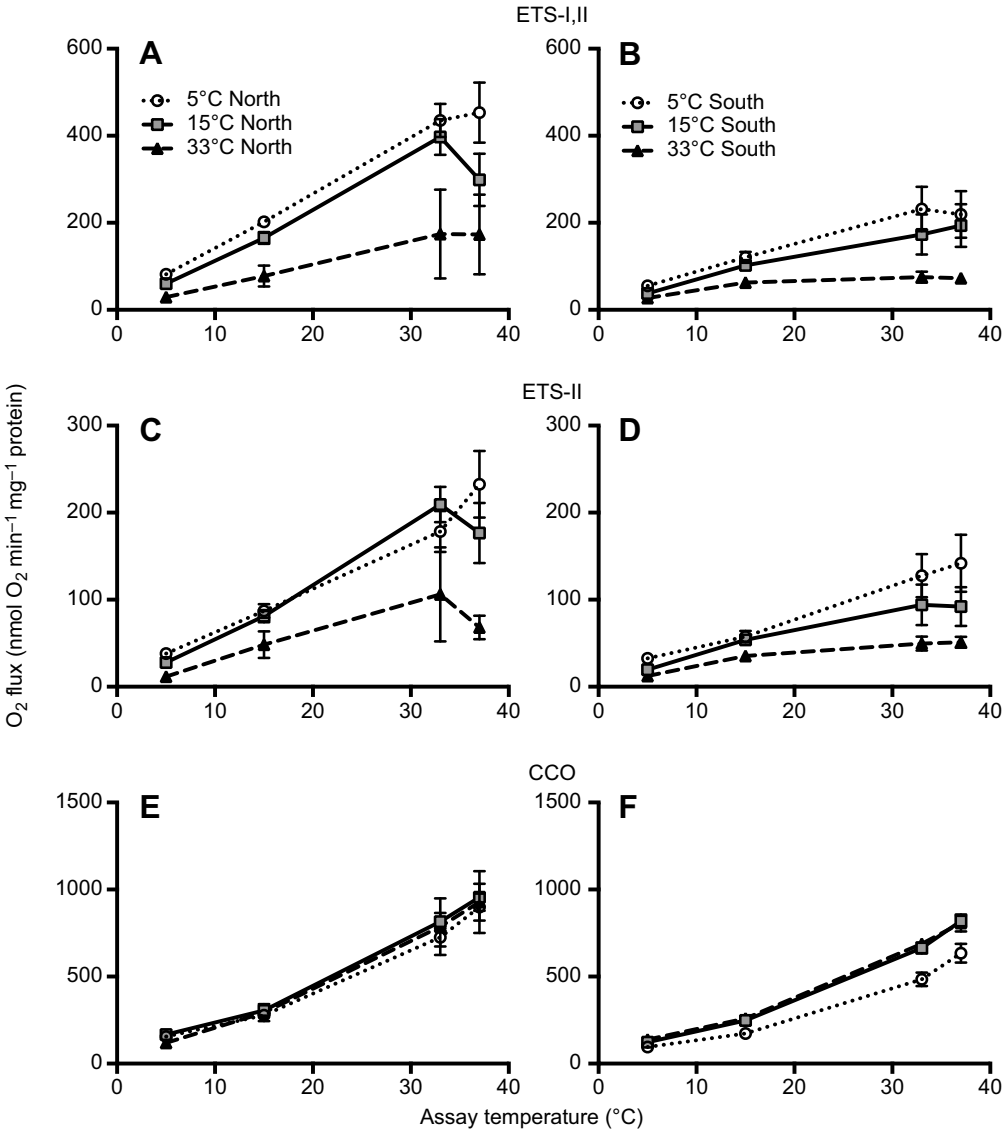

Fig. 2. Maximum liver mitochondrial respiratory capacity. Northern (A,C,E) and southern (B,D,F) *F. heteroclitus* were acclimated to 5, 15 or 33°C for 4 weeks. Substrate oxidation capacity (ETS) was fueled through electron transport system complexes I and II simultaneously (A,B; pyruvate, malate, glutamate and succinate as substrates) or complex II alone (C,D; succinate as a substrate). Apparent cytochrome *c* oxidase (CCO) capacity (E,F) was determined in an uncoupled state. Data are means±s.e.m., see Table 1 for associated statistics (n=7–8 pooled samples, with 7 individuals per pool).

Journal of Experimental Biology (2018) 221, jeb174458. doi:10.1242/jeb.174458

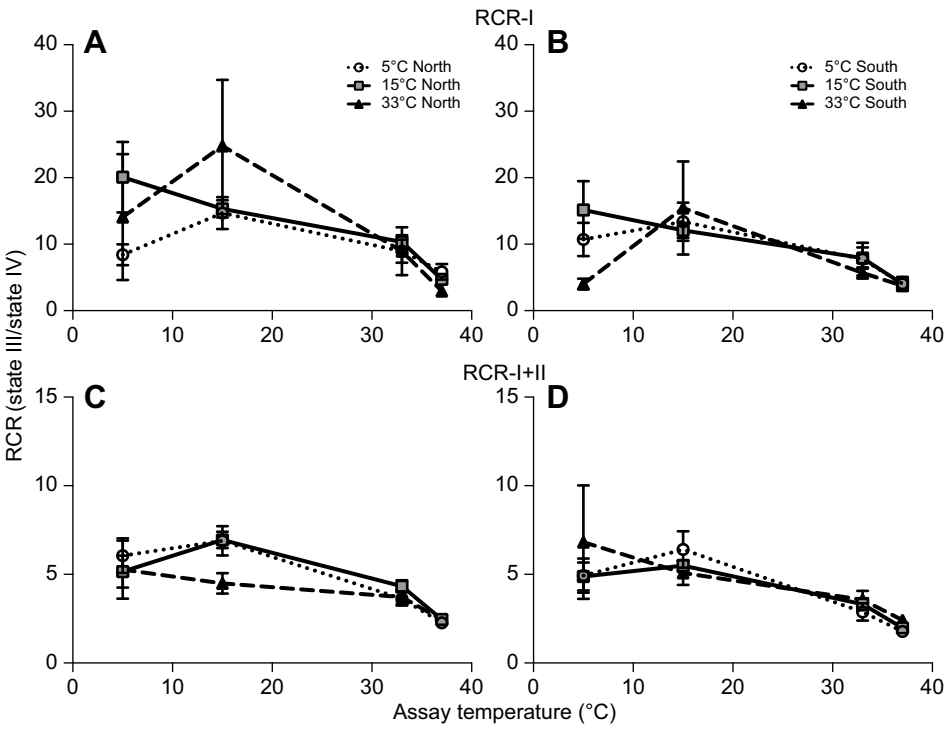

Fig. 3. Liver mitochondrial apparent respiratory control ratios (RCRs). Northern (A,C) and southern (B,D) *F. heteroclitus* were acclimated to 5, 15 or 33°C for 4 weeks. RCRs were calculated from respiratory flux fueled with electron transport system complex I (A,B; pyruvate, malate, glutamate as fuels) or complexes I and II simultaneously (C,D; complex I substrates and succinate). Data are means±s.e.m., see Table 1 for associated statistics (n=7–8 pooled samples, with 7 individuals per pool).

Mitochondrial phospholipids

To determine whether the observed variation in mitochondrial function between subspecies and acclimation temperatures was paralleled by changes in mitochondrial membrane composition, we performed a comprehensive analysis of mitochondrial phospholipid class distribution, fatty acid composition and cardiolipin molecular species profile. Principal component analyses were initially employed to describe overall patterns of variation and revealed acclimation temperature as the strongest modifier of mitochondrial membrane composition (Fig. 4A). Principal component 1 accounted for 35.5% of the total variation and fully separated thermal acclimation treatments (Fig. 4B, $P_{\text{acclimation}}<1.06\times10^{-11}$), but did not account for subspecies variation ($P_{\text{subspecies}}=0.067$) or its interaction with thermal acclimation ($P_{\text{acclimation}\times\text{subspecies}}=0.087$). Principal component 3 (9.1% of total phospholipid variation) separated northern and southern *F. heteroclitus* ($P_{\text{subspecies}}<0.001$) and thermally acclimated fish ($P_{\text{acclimation}}<0.001$), but there was an interaction between these factors ($P_{\text{acclimation}\times\text{subspecies}}=2.11\times10^{-5}$) driven by the lack of subspecies differences following 33°C acclimation (Fig. 4C). Principal component 2 (16.2% of total phospholipid variation) did not account for the effects of thermal acclimation or subspecies (Fig. S2; $P_{\text{acclimation}}=0.687$, $P_{\text{subspecies}}=0.236$, $P_{\text{acclimation}\times\text{subspecies}}=0.230$).

To identify the specific aspects of mitochondrial membrane composition most responsible for thermal acclimation responses and subspecies variation, we evaluated the contribution of each individual membrane feature to principal components 1 and 3 (Table S1). Changes in cardiolipin molecular species represented 15 of 20 strongest contributors to trends in PC1 (48% of total contribution), with PE fatty acids being the next most robust variants (30% of total contribution). Similar trends were seen in principal component 3, with particularly strong contributions of monolyso-CL (MLCL) species and unsaturated PE fatty acids. Therefore, we next evaluated the direction of changes in phospholipid class distribution, specific CL molecular species, and phospholipid fatty acid characteristics (Fig. 5).

Acclimation temperature altered mitochondrial phospholipid class distribution differently in northern compared with southern *F. heteroclitus* (Fig. 5A; Table S2). Acclimation from 15°C to either 5°C or 33°C tended to decrease membrane PC and increase PE content in northern *F. heteroclitus*, whereas southern subspecies showed the opposite trend. CL content tended to increase with lower acclimation temperatures in both subspecies, with more pronounced effects in the southern subspecies. Reciprocal changes in MLCL levels at least partially implicate altered CL acyl chain hydrolysis or esterification in these CL content variations, particularly in the southern subspecies.

Acclimation temperature induced changes in the CL molecular species profile that were largely consistent between subspecies (Fig. 5B; Tables S2 and S3). Lower temperatures tended to decrease CL 18:2n6 enrichment, and favored greater incorporation of 20:4n6 (arachidonic acid) and 18:1 (oleic or vaccenic acid). Similar trends were seen in the total mitochondrial phospholipid fatty acid profile (Fig. 5C; Table S4), with particularly marked increases in 18:1n7 (vaccenic acid), but not 18:1n9 (oleic acid), following acclimation to colder temperatures. Vaccenic acid has been reported to be the predominant form of 18:1 present in CL, but its physiological role in mitochondrial membranes has remained unclear. The fatty acid composition of PC and particularly PE also varied with acclimation temperature (Fig. 5A, Tables S5 and S6), with class-specific changes reflecting the selectivity of phospholipid remodeling enzymes and perhaps an exchange of FAs to CL molecular species (Schlame, 2013). Whereas phospholipid saturated fatty acids tended to decline with colder acclimation temperatures, general membrane phospholipid characteristics such as the FA double-bond index (DBI) and chain length remained relatively stable in both subspecies (Fig. 5D, Table S7). However, consistent trends for higher n6 and n7 FAs were seen in both species, largely reflecting the increases in 20:4n6 and 18:1n7.

Reciprocal changes in phospholipid FAs leading to higher levels of non-essential unsaturated species suggest that FA desaturase and elongase enzymes might contribute to variations in phospholipid

Journal of Experimental Biology (2018) 221, jeb174458. doi:10.1242/jeb.174458

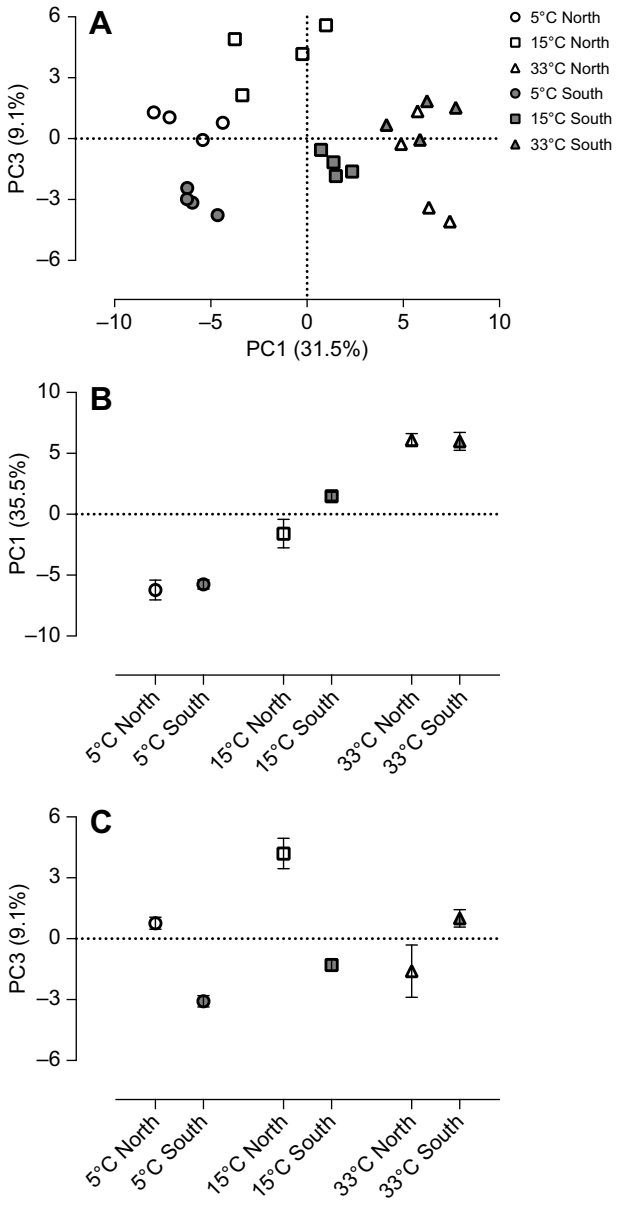

Fig. 4. First and third principal component scores for liver mitochondrial membrane composition of thermally acclimated *F. heteroclitus*. Northern (white symbols) and southern (gray symbols) *F. heteroclitus* were acclimated to 5, 15 or 33°C for 4 weeks. (A) Plot of individuals along PC1 and PC3 axes. (B) Individual values extracted from PC1 significantly separated thermal acclimation treatments. (C) Individual values extracted from PC3 significantly separated both thermal acclimation and subspecies treatments. See Results for associated statistics, n=4 pooled samples, with 7 individuals per pool.

composition observed following acclimation to colder temperatures. Consistent with this prediction, FA product/precursor ratios corresponding to n6 and n3 Δ6-desaturase (D6D), 16C stearoyl-CoA desaturase (SCD) and FA elongase-6 (ELOVL6) activities were all highest following acclimation to 5°C in both northern and southern *F. heteroclitus* (Fig. 6A, Table S8). Opposite patterns of *de novo* 18:0 synthesis and desaturation (by ELOVL6 and SCD, respectively) were observed between northern and southern subspecies, but no other marked intraspecific variation in thermal acclimation responses was evident. Integration of trends observed for all FAs within established biosynthesis pathways indicates that a distinct pattern of long-chain FAs is favored in mitochondrial membranes in response to colder temperatures (Fig. 6B). This pattern is dominated by increases in 18:1n7, 20:4n6 and 22:6n3 in both northern and southern subspecies, despite differences between subspecies in general membrane characteristics (Fig. 5A,D).

Inner mitochondrial membrane content

We estimated thermal acclimation and subspecies effects on IMM content by comparing cardiolipin content normalized to mg mitochondrial protein (Fig. 7A). In addition, we assessed thermal acclimation and subspecies effects on LEAK-I+II; OXPHOS-I+II and ETS-I+II respiratory capacity normalized to CCO capacity (Fig. 7B-D). Cardiolipin content was greatest following low-temperature acclimation temperature and in the northern subspecies ($P_{acclimation}$<0.001, $P_{subspecies}$<0.005). This subspecies effect was removed following 33°C acclimation ($P_{interaction}$<0.005).

Respiratory capacity normalized to CCO capacity

Mitochondrial respiratory capacities (i.e. LEAK-I+II, OXPHOS-I+II and ETS-I+II) normalized to CCO capacity increased with decreasing acclimation temperature ($P_{acclimation}$<0.001). Northern *F. heteroclitus* exhibited greater OXPHOS-I+II ($P_{subspecies}$<0.01) and ETS-I+II ($P_{subspecies}$<0.05) respiratory capacity that was normalized to CCO capacity, but the subspecies did not differ for LEAK-I+II/CCO ($P_{subspecies}$=0.791). No significant interaction effects (i.e. subspecies×acclimation) were detected (P_{LEAK}=0.739, P_{OXPHOS}=0.467, P_{ETS}=0.141).

DISCUSSION

The present study provides a comprehensive analysis of mitochondrial performance and membrane composition following thermal acclimation of two locally adapted subspecies of *F. heteroclitus*. Results support a role for parallel changes in these parameters to maintain bioenergetic homeostasis in response to thermal stress and identify novel intraspecific patterns of mitochondrial membrane remodeling under these conditions. We suggest that particular aspects of mitochondrial function and lipid metabolism are targeted by selection and contribute to the eurythermal physiology of this species.

Intraspecific variation in mitochondrial performance

A primary objective of this study was to determine if putatively locally adapted *F. heteroclitus* subspecies exhibit differences in liver mitochondrial performance that might underlie established differences in organismal aerobic metabolism and associated traits (e.g. thermal and hypoxia tolerance limits). Our results clearly demonstrate a greater hepatic mitochondrial respiratory capacity of northern versus southern *F. heteroclitus*, which is consistent with greater aerobic metabolic rates in northern subspecies (Fangue et al., 2009; Healy and Schulte, 2012). However, previous studies have produced mixed evidence for intraspecific variation of mitochondrial function in *F. heteroclitus*. This may be a consequence of different tissues being utilized in different studies, as there is no evidence of increased mitochondrial respiratory capacity in the heart or brain in northern killifish (Baris et al., 2016; Chung et al., 2017a). Indeed, subspecies differences in *F. heteroclitus* liver mitochondrial performance are not always detected (Fangue et al., 2009). This could be due to the specific population being studied, given the genetic variation present within *F. heteroclitus* subspecies (McKenzie et al., 2016). Alternatively, differences in the substrate combinations used to assay mitochondrial function could explain the differences in findings

Journal of Experimental Biology (2018) 221, jeb174458. doi:10.1242/jeb.174458

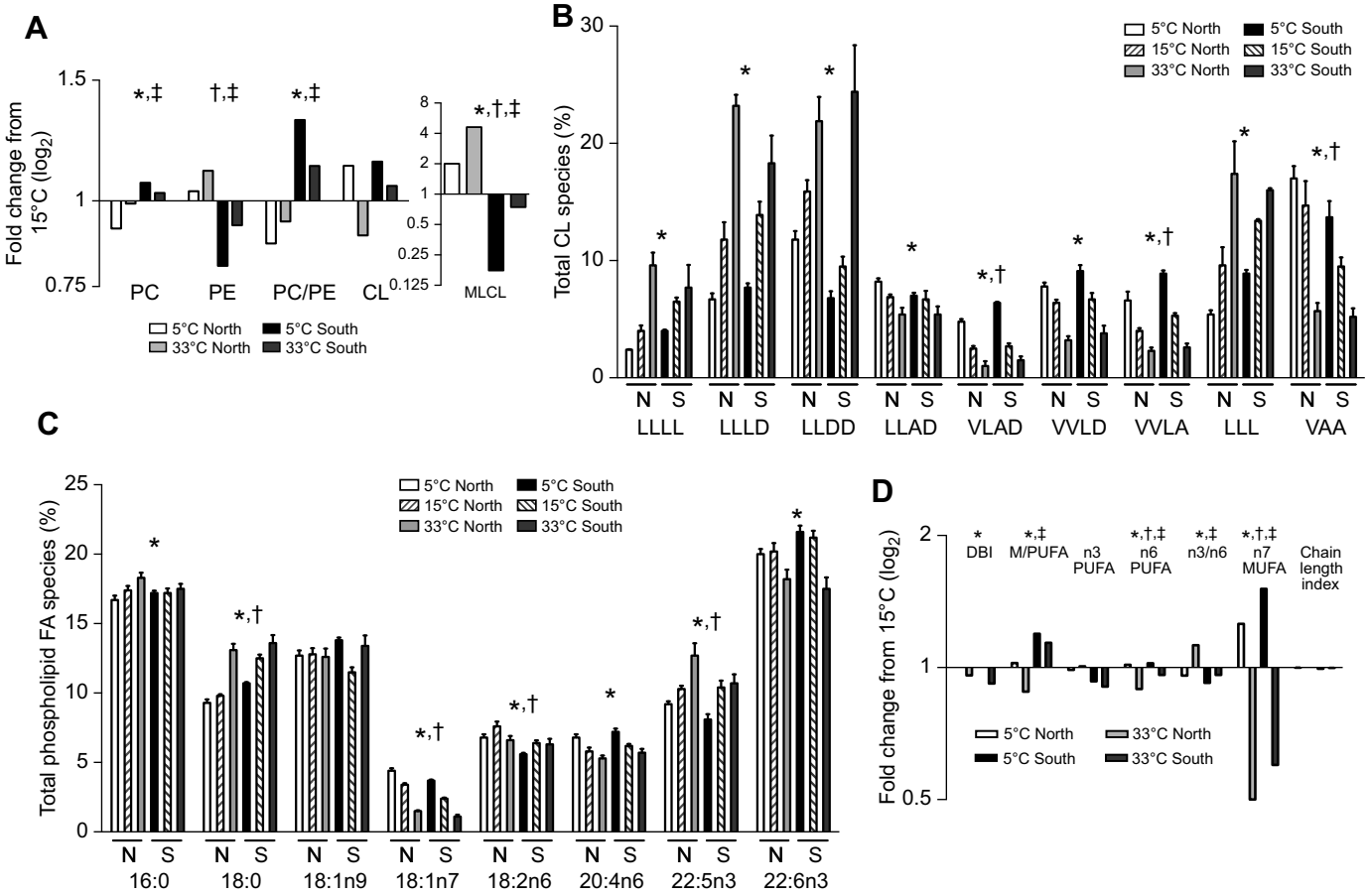

Fig. 5. Mitochondrial membrane remodeling in response to thermal stress. (A) Fold changes in mitochondrial phosphatidylcholine (PC), phosphatidylethanolamine (PE), the PC/PE ratio, cardiolipin (CL), and monolyso CL (MLCL) content in response to 5°C and 33°C acclimation relative to 15°C. (B) Predominant cardiolipin molecular species from northern (N) and southern (S) *F. heteroclitus* changed following acclimation to 5, 15 and 33°C. The fatty composition of tetra-acyl (4 letters) or mono-lyso (3 letters) CL species are indicated by L (18:2n6, linoleic), D (22:6n3, docosahexaenoic), A (20:4n6, arachidonic) and V (18:1n7, vaccenic). (C) Predominant fatty acids extracted from total mitochondrial phospholipids following acclimation to 5, 15 and 33°C. (D) Fold changes in general characteristics of total mitochondrial phospholipid fatty acid profile in response to 5°C and 33°C acclimation relative to 15°C. DBI, double bond index; M/PUFA, the ratio of monounsaturated FA to polyunsaturated FA. Symbols indicate significant effects from a two-way ANOVA comparing associated mean values (see Table 1 for mean values and sample size). *Acclimation; †subspecies; ‡acclimation×subspecies. See relevant table for sample size (Tables S1–S7).

between these studies. Our use of multiple substrates and populations from the extreme ends of the species distribution appears to provide the resolution necessary to detect subspecies variation in liver mitochondrial respiratory capacity.

Whole-organism hypoxia tolerance limits are thought to be shaped by declines in aerobic metabolism and associated mitochondrial failure (Deutsch et al., 2015; Fry and Hart, 1948; Pörtner, 2001). Our demonstration of lower mitochondrial capacity in southern *F. heteroclitus* is consistent with greater hypoxia tolerance in this subspecies (McBryan et al., 2016). Putative links between mitochondrial function and hypoxia tolerance may extend to thermal tolerance as these limits are thought to be a consequence of temperature induced systemic hypoxemia (Pörtner, 2001). Northern and southern *F. heteroclitus* exhibit thermal tolerance limits that are consistent with their northern temperate geographic distributions (Fangue et al., 2006). A lower mitochondrial capacity in the southern subspecies may reflect a lower tissue metabolic and O_2 demand, due to regulated metabolic suppression allowing for sustained performance at high-temperatures. Alternatively, the greater mitochondrial capacity exhibited by northern *F. heteroclitus* may help to sustain ATP production and thus maintain aerobic performance at lower temperatures.

Thermal acclimation effects on mitochondrial respiratory capacity

Thermal acclimation responses of ectotherms may involve changes in mitochondrial performance to maintain bioenergetic homeostasis (Guderley, 2011). Our demonstration of an increase in mitochondrial respiratory capacity following low-temperature acclimation in both northern and southern *F. heteroclitus* is consistent with a previous report in northern subspecies (Chung and Schulte, 2015). Low-temperature acclimation is associated with increased mitochondrial function in other ectotherms (Dos Santos et al., 2013; Kraffe et al., 2007), perhaps reflecting a compensation for slower biochemical reaction rates in low temperatures. Although we observe a pattern of increased respiratory capacity with low-temperature acclimation, the magnitude of this effect is not large. This may indicate that the maintenance of energetic balance following thermal acclimation requires the recruitment of mechanisms such as increases in mitochondrial volume density (Dhillon and Schulte, 2011; St-Pierre et al., 1998) as well as increases in capacity.

In contrast to low-temperature effects, high-temperature acclimation decreased mitochondrial respiratory capacity. This might represent beneficial acclimation as acute increases in temperature may result in unsustainable biochemical reaction rates

Journal of Experimental Biology (2018) 221, jeb174458. doi:10.1242/jeb.174458

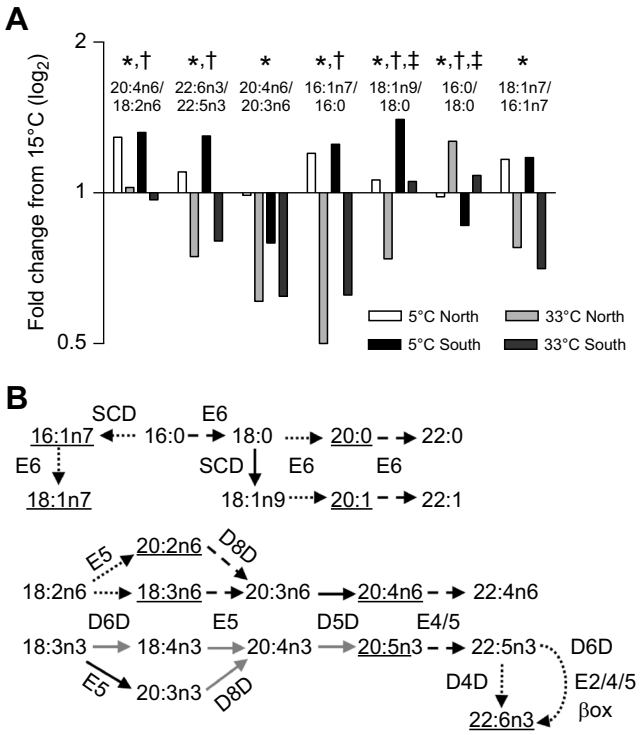

Fig. 6. Mitochondrial membrane fatty acid desaturase and elongase product/precursor ratios. (A) Fold changes in selected fatty acid product/precursor ratios from total mitochondrial phospholipids in response to 5°C and 33°C acclimation relative to 15°C in northern and southern *F. heteroclitus*. (B) Predominant pathways of long-chain fatty acid desaturation and elongation. Fatty acids and membrane remodeling enzymes are indicated to illustrate those that tended to be highest at 5°C (underlined FAs, black dotted arrow), highest at 33°C (bold FAs, black dashed arrow), not uniformly respond to acclimation temperature (black unformatted FAs, solid black arrow), or were not detected (gray unformatted FAs, solid gray arrow). Enzymes are listed for each reaction include E, elongase; D6D, Δ-6 desaturase; D5D, Δ-5 desaturase; D4D, Δ-4 desaturase; D8D, Δ-8 desaturase; SCD, stearoyl-CoA desaturase; βox, β-oxidation. Symbols indicate significant effects from a two-way ANOVA comparing associated mean values (see Table S8 for mean values). *: acclimation; †: subspecies; ‡: acclimation×subspecies. n=7–8 pooled samples, with 7 individuals per pool.

and generation of reactive oxygen species (Abele et al., 2002). Decreased mitochondrial function with high-temperature acclimation has been previously reported in *F. heteroclitus* and other aquatic ectotherms (Chung and Schulte, 2015; Khan et al., 2014; Kraffe et al., 2007; Strobel et al., 2013). Although our observed decrease in mitochondrial function could be consistent with a beneficial high-temperature response, they might alternatively be a consequence of sub-lethal stress (Chung and Schulte, 2015; Chung et al., 2017a). Indeed, we found that 33°C acclimation is associated with decreased whole-organism and liver mass. But acclimation to 33°C is not lethal over prolonged periods (Fangue et al., 2006), suggesting that this temperature represents a sub-lethal stressor. The effect of sub-lethal temperature stress on teleost mitochondrial function is a relatively unexplored area of research with large implications for our understanding of species' fitness (Iles, 2014; Lemoine and Burkepile, 2012; Salin et al., 2016).

Changes in mitochondrial performance following thermal acclimation were not clearly associated with a single ETS component (Figs 1 and 2, Fig. S1). However, it should be noted that our use of substrate combinations (ETS CI and CII simultaneously) can make it difficult to disentangle the involvement of CII in the thermal acclimation response. But maximum ETS flux through CII (ETS-II; Fig. 2C,D) exhibited a pattern similar to both CI and CI+CII-linked respiration which indicates that this is a broad-scale thermal acclimation response. In contrast, thermal acclimation did not alter apparent CCO capacity (Fig. 2E,F). Indicating that thermal acclimation specifically alters ETS performance upstream of CCO, perhaps through CI (Chung and Schulte, 2015). But this effect is not universal across fishes, as increased acclimation temperature has been shown to decrease CCO activity in *Onchorynchus mykiss* (Kraffe et al., 2007). Nevertheless, thermal acclimation may alter CCO function as we have noted thermal acclimation effects on mitochondrial O_2 binding affinity in this species (Chung et al., 2017b). Taken together, the effects of thermal acclimation on mitochondrial performance are consistent with the maintenance of biochemical reaction rates in response to temperature effects. The observed changes demonstrate the importance of maintaining mitochondrial function in the face of prolonged thermal stress and likely underlie the eurythermal physiology of this species.

Thermal acclimation and intraspecific effects on mitochondrial membrane composition

The present study demonstrates variation in mitochondrial membrane composition between *F. heteroclitus* subspecies that changed in parallel with respiratory function following thermal acclimation. Thermal acclimation induced the largest changes in mitochondrial membrane composition (principal component 1), primarily due to shifts in phospholipid FAs. Subspecies effects accounted for less total variation in mitochondrial membrane composition (principal component 3) and were largely associated with variation in phospholipid class distribution and a smaller set of unsaturated FAs. Both subspecies exhibited similar responses to thermal acclimation for the majority of mitochondrial membrane characteristics. Our findings indicate that changes in phospholipid FA composition are the primary signature of thermal acclimation in hepatic mitochondrial membranes, whereas shifts in phospholipid classes are more closely associated with putative local adaptation responses. These responses were observed in fish held under common conditions in the laboratory. In nature, the northern and southern subspecies may have access to different prey items and these prey items may differ among seasons. It is therefore possible that natural populations may differ in lipid composition to an even greater extent than observed here. However, our data clearly show that the northern and southern populations differ in their mitochondrial membrane composition, and express the ability to modify membrane composition with thermal acclimation, even when fed a common diet.

Phosphatidylcholine (PC) and phosphatidylethanolamine (PE) comprise the majority of phospholipids present in mitochondria, and changes in their relative proportions (i.e. PC/PE ratio) have been associated with altered membrane fluidity following thermal acclimation (Hazel and Landrey, 1988). In the present study, the PC/PE ratio was similar between *F. heteroclitus* subspecies acclimated to 15°C but tended to increase in the southern subspecies in response to either 5°C or 33°C acclimation, and decrease in the northern subspecies under the same conditions. These opposing responses suggest distinct strategies between the subspecies for coping with thermal stress (rather than cold or heat, per se) through modulation of mitochondrial phospholipid metabolism. Moderate (<30%) decreases in mitochondrial PE (leading to higher PC/PE) result in a less fluid membrane environment (Li et al., 2006), and can alter cristae morphology

Journal of Experimental Biology (2018) 221, jeb174458. doi:10.1242/jeb.174458

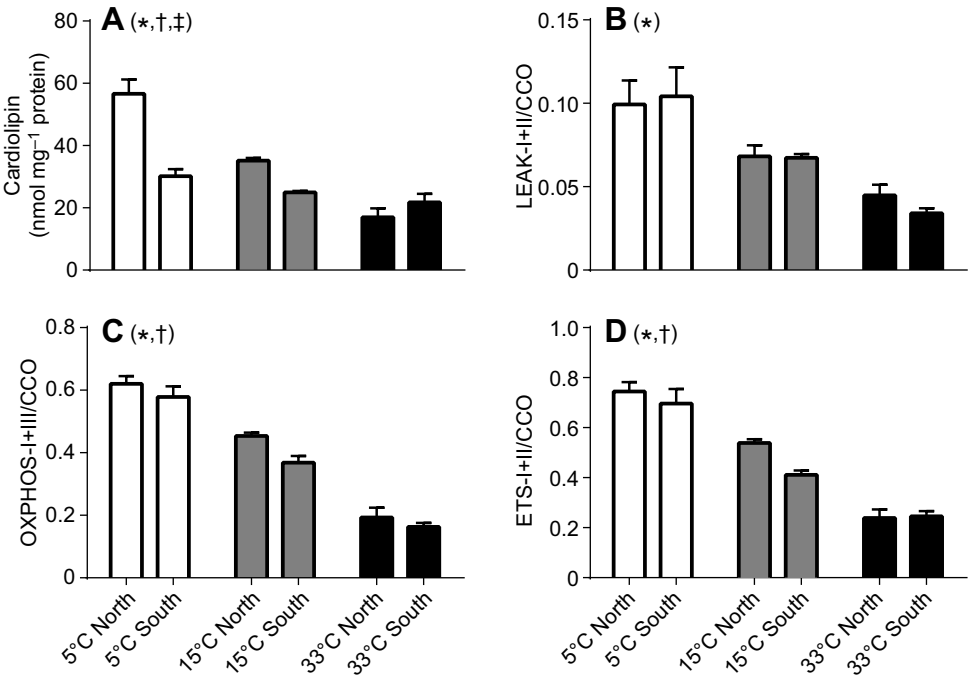

Fig. 7. Estimates of thermal acclimation and subspecies effects on inner mitochondrial membrane content and associated enzymes. Northern and southern *F. heteroclitus* were acclimated to 5, 15 and 33°C for 4 weeks. (A) Whole mitochondrial cardiolipin content normalized to mg mitochondrial protein. (B) LEAK respiration normalized to apparent cytochrome *c* oxidase (CCO) capacity. (C) Oxidative phosphorylation (OXPHOS) respiration normalized to CCO capacity. (D) Substrate oxidation capacity (ETS) normalized to CCO capacity. LEAK, OXPHOS and ETS were fueled through electron transport system complexes I and II simultaneously (I+II; pyruvate, malate, glutamate and succinate as substrates). Data are means±s.e.m., symbols indicate significant effects from a two-way ANOVA (*acclimation; †subspecies; ‡acclimation×subspecies, *n*=7–8 pooled samples, with 7 individuals per pool).

and reduce respiratory capacity (Tasseva et al., 2013). Conversely, a 33% increase in hepatic mitochondrial PC/PE has been associated with higher respiration and ATP production (van der Veen et al., 2014). Our observed variation in phospholipid classes is consistent with these studies as the southern subspecies, which has lower respiratory capacity, exhibited lower mitochondrial PE compared with levels in the northern subspecies following acclimation to 5°C or 33°C. However, this does not explain the functional differences between the subspecies acclimated to 15°C where PE and PC/PE were similar between subspecies. It is important to note that the global PC/PE ratio describes variation in total phospholipid classes and does not differentiate among phospholipid subclasses (e.g. diacyl-, lyso- and plasmalogen species). Kraffe et al. (2007) demonstrate that phospholipid classes vary following thermal acclimation in a subclass-specific manner. Although not investigated here, variation in these mitochondrial phospholipid subclasses likely contributes to the thermal acclimation response in both subspecies and has implications for membrane properties beyond changes in fluidity. Notably, reciprocal changes in PE and PC often reflect changes in PE methyltransferase (PEMT) activity, which converts PE to PC by N-methylation and is a potent regulator of hepatic lipoprotein assembly, choline metabolism and gluconeogenesis (Vance et al., 2007, van der Veen et al., 2014).

In addition to PE and PC, the IMM contains the unique dimeric phospholipid cardiolipin (CL), which is known to be critical for maintaining membrane integrity and organelle function (Schlame, 2007). Consistent with previous observations in *O. mykiss* acclimated to a range of temperatures (Kraffe et al., 2007), CL content expressed as a percentage of total lipids did not change significantly in response to thermal acclimation or between subspecies in the present study. However, there were substantial changes in monolysocardiolipin (MLCL) with thermal acclimation in both subspecies that generally reflected reciprocal (non-significant) changes in CL content. The direction of these changes varied between subspecies, with MLCL being highest at 5°C in the northern and at 15°C in the southern subspecies, suggesting intraspecific variation in CL deacylation/reacylation in response to thermal stress (Taylor et al., 1999). Indeed, marked changes in CL acyl chain composition were observed across acclimation temperatures, indicating significant induction of CL remodeling pathways.

Decreasing acclimation temperature tended to decrease the proportion of CL species enriched with 18:2n6, and increase those containing 18:1, 20:4n6 and 22:6n3 in both *F. heteroclitus* subspecies. A similar pattern of CL remodeling was reported in muscle mitochondria from *O. mykiss* following cold acclimation (Kraffe et al., 2007), which was suggested as the potential mechanism underlying changes in respiratory capacity across acclimation temperature in this species. Compositional changes in CL generally paralleled FA shifts in the total mitochondrial phospholipid fraction in the present study, but varied somewhat from those observed in PE and PC, suggesting a preferential enrichment of CL 18:1n7, 20:4n6 and 22:6n3 at colder temperatures. These increases in unsaturated fatty acids may help to preserve mitochondrial membrane fluidity at colder temperatures in accordance with HVA (Hazel, 1995), but were largely balanced by changes in 18:2n6 and 22:5n3 that maintained a similar membrane double-bond index across acclimation temperatures. Therefore, we postulate that shifts in the content of particular FAs or their phospholipid esterification may serve more specific roles in regulating mitochondrial physiology, and perhaps reflect broader changes in cellular lipid metabolism relevant to organismal thermal adaptation. For example, changes in membrane 22:6n3 content have been associated with a wide array of metabolic phenotypes that likely involve effects other than a contribution to membrane unsaturation (Hagve et al., 2009; Leray et al., 1984; Muriana et al., 1992; Stillwell and Wassall, 2003). Thus, our data are more consistent with a targeted mitochondrial membrane remodeling as opposed to a general shift in membrane composition to maintain fluidity (Hazel, 1995; Kraffe et al., 2007).

The relative contents of selected membrane FAs are often used to estimate the *in vivo* activity of various desaturase and elongase

enzymes involved in the biosynthesis of long-chain unsaturated fatty acids, which are predominantly esterified to membrane phospholipids. Thermal acclimation altered indices associated with three such enzymes, highlighting plausible mediators of the observed alterations in membrane FA composition. In particular, the accumulation of 20:4n6 and 22:6n3 following decreased acclimation temperature was associated with decreases in their FA precursors (18:2n6 and 22:5n3), suggesting an increase in both n3- and n6-PUFA delta-6 desaturase (Δ6D) activity following acclimation to low temperatures in both subspecies. Δ6D catalyzes critical rate-limiting steps in the synthesis of long-chain highly unsaturated PUFAs (Fig. 6B), and thus has been linked to a wide range of physiological and pathological phenotypes (Tosi et al., 2014). Δ6D has also been implicated in teleost responses to low temperature and salinity, but little is known about its regulation in the context of thermal acclimation (Santigosa and Vagner, 2011).

Decreasing acclimation temperature also increased the 16:1n7/16:0 index of stearoyl-CoA desaturase (SCD) activity in both *F. heteroclitus* subspecies, which along with the conversion of 18:0 to 18:1n9, provides the major source of *de novo*-synthesized monounsaturated FAs from saturated FAs (Paton and Ntambi, 2009). This increase in the membrane content of monounsaturated/saturated FAs favors an increase in fluidity that is consistent with HVA to colder temperatures (Guderley, 2004). Increases in SCD activity might also regulate broader aspects of hepatic function and metabolism, including triglyceride biosynthesis, glucose utilization, inflammation and stress response (Liu et al., 2011). In addition, the SCD product 16:1n7 can be elongated by ELOVL6 to 18:1n7, which increased dramatically in response to colder temperatures, along with other indices of ELOVL6 activity. In contrast to decreases in FA saturation, longer FA chains are associated with decreased membrane fluidity (Marsh, 2010). However, average membrane FA chain length was not altered following thermal acclimation in the present study, suggesting a more specialized role of ELOVL6 toward specific substrates, or metabolism of selected products by other enzymes downstream. Interestingly, ELOVL6 activity increases with cold exposure in mice and is essential for maintaining mitochondrial capacity and thermogenic function in brown adipose tissue (Virtue et al., 2015). Given the parallel increases in mitochondrial membrane 18:1n7 and respiratory capacity in cold-acclimated fish in the present study, the potential roles of SCD and ELOVL6 in regulating mitochondrial function in poikilotherms merits further investigation.

Inner mitochondrial membrane content and variation in mitochondrial respiration

Although we suggest that mitochondrial membrane composition alters the intrinsic function of the OXPHOS apparatus, thermal acclimation and intraspecific effects on mitochondrial respiratory capacity could be due to changes in total IMM content and its associated enzymes. To investigate this possibility, we compared thermal acclimation and intraspecific effects on absolute cardiolipin content normalized to total mitochondrial protein content and mitochondrial respiratory capacities normalized to CCO capacity (T_{assay}=15°C; Fig. 7). Cardiolipin content was greater in the northern subspecies and increased following cold acclimation, a pattern that was similar to variation in mitochondrial respiratory capacity (Fig. 1). This suggests that much of the difference in respiratory capacity between subspecies and with acclimation could be due to changes in the amount of IMM per mitochondrion. Consistent with this hypothesis, subspecies effects on CCO normalized mitochondrial respiratory capacity were smaller relative to those observed for respiratory capacity normalized to mitochondrial protein content. However, clear acclimation effects remained even when respiratory capacity is normalized to CCO capacity. Maximum CCO capacity did not change significantly with thermal acclimation (Fig. 2E,F) whereas thermal acclimation had strong effects on other components of the ETS. These data indicate that variation in IMM content partially accounts for our observed thermal acclimation and intraspecific variation effects on mitochondrial respiratory capacity, but that CCO capacity does not change in parallel. In general, CCO capacity is thought not to be limiting for ETS function (Gnaiger et al., 1998), and our data are consistent with this pattern. Taken together, a substantial component of the differences in respiratory capacity between subspecies and acclimation temperatures can be accounted for by changes in IMM amount, but we detected significant intraspecific and thermal acclimation effects on CCO-normalized mitochondrial respiratory capacity, which supports a role for mechanisms in addition to changes in IMM content in driving changes in mitochondrial function.

Our data provide support for mitochondrial membrane remodeling as a mechanism driving variation in mitochondrial performance following thermal acclimation and local adaptation. Respiratory capacity increased in response to decreasing acclimation temperature and was greater in the putatively cold-adapted northern subspecies. This variation in mitochondrial respiration is consistent with previously observed whole-organism responses to thermal acclimation and intraspecific variation of aerobic metabolism. We demonstrate a targeted remodeling of mitochondrial phospholipids in response to acclimation and differences in membrane phospholipid composition between subspecies, indicating that *F. heteroclitus* utilizes regulated membrane remodeling as a response to thermal stress at multiple timescales. In addition, both thermal acclimation and putative local adaptation to cold temperatures were associated with greater estimates of IMM content, which partly accounts for our observed variation in mitochondrial respiratory capacity. The ability to remodel mitochondrial membrane phospholipids and alter respiratory capacity likely underlies the highly eurythermal physiology of these fish and may have been a target of natural selection.

Acknowledgements

A. Cooper, K. Crowther, T. Healy, B. Marshall for assistance with animal sampling and H. Bryant for assistance with experiments.

Competing interests

The authors declare no competing or financial interests.

Author contributions

Conceptualization: D.J.C., P.M.S.; Methodology: D.J.C., A.J.C.; Formal analysis: D.J.C.; Investigation: D.J.C., G.C.S.; Writing - original draft: D.J.C.; Writing - review & editing: D.J.C., G.C.S., A.J.C., P.M.S.; Visualization: D.J.C., A.J.C.; Supervision: P.M.S.; Funding acquisition: A.J.C., P.M.S.

Funding

Funding was provided by a Natural Sciences and Engineering Research Council of Canada Discovery grant to P.M.S., a Canada Graduate Scholarship and a Michael Smith Foreign Study Supplement (MSFSS); a Journal of Experimental Biology traveling fellowship to D.J.C.; U.S. Department of Agriculture National Institute of Food and Agriculture and an American Heart Association grant to A.J.C.

Supplementary information

Supplementary information available online at
http://jeb.biologists.org/lookup/doi/10.1242/jeb.174458.supplemental

References

Abdi, H. and Williams, L. J. (2010). Principal component analysis. *WIREs Comp. Stat.* **2**, 433-459.

Abele, D., Heise, K., Pörtner, H. O. and Puntarulo, S. (2002). Temperature-dependence of mitochondrial function and production of reactive oxygen species in the intertidal mud clam *Mya arenaria*. *J. Exp. Biol.* **205**, 1831-1841.

Archer, S. D. and Johnston, I. A. (1991). Density of cristae and distribution of mitochondria in the slow muscle fibers of Antarctic fish. *Physiol. Zool.* **64**, 242-258.

Baris, T. Z., Crawford, D. L. and Oleksiak, M. F. (2016). Acclimation and acute temperature effects on population differences in oxidative phosphorylation. *Am. J. Physiol. Regul. Integr. Comp. Physiol.* **310**, R185-R196.

Bradford, M. M. (1976). A rapid and sensitive method for the quantitation of microgram quantities of protein utilizing the principle of protein-dye binding. *Anal. Biochem.* **72**, 248-254.

Caldwell, R. S. and Vernberg, F. J. (1970). The influence of acclimation temperature on the lipid composition of fish gill mitochondria. *Comp. Biochem. Physiol.* **34**, 179-191.

Chicco, A. J. and Sparagna, G. C. (2007). Role of cardiolipin alterations in mitochondrial dysfunction and disease. *Am. J. Physiol. Cell. Phys.* **292**, C33-C44.

Chung, D. J. and Schulte, P. M. (2015). Mechanisms and costs of mitochondrial thermal acclimation in a eurythermal killifish (*Fundulus heteroclitus*). *J. Exp. Biol.* **218**, 1621-1631.

Chung, D. J., Bryant, H. J. and Schulte, P. M. (2017a). Thermal acclimation and subspecies-specific effects on heart and brain mitochondrial performance in a eurythermal teleost (*Fundulus heteroclitus*). *J. Exp. Biol.* **220**, 1459-1471.

Chung, D. J., Morrison, P. R., Bryant, H. J., Jung, E., Brauner, C. J. and Schulte, P. M. (2017b). Intraspecific variation and plasticity in mitochondrial oxygen binding affinity as a response to environmental temperature. *Sci. Rep.* **7**, 16238.

Crockett, E. L., Dougherty, B. E. and McNamer, A. N. (2001). Effects of acclimation temperature on enzymatic capacities and mitochondrial membranes from the body wall of the earthworm *Lumbricus terrestris*. *Comp. Biochem. Physiol. B* **130**, 419-426.

Dahlhoff, E. A. and Somero, G. N. (1993). Effects of temperature on mitochondria from abalone (genus *Haliotis*): adaptive plasticity and its limits. *J. Exp. Biol.* **185**, 151-168.

Deutsch, C., Ferrel, A., Seibel, B., Pörtner, H.-O. and Huey, R. B. (2015). Climate change tightens a metabolic constraint on marine habitats. *Science* **348**, 1132-1135.

Dhillon, R. S. and Schulte, P. M. (2011). Intraspecific variation in the thermal plasticity of mitochondria in killifish. *J. Exp. Biol.* **214**, 3639-3648.

Dos Santos, R. S., Galina, A. and Da-Silva, W. S. (2013). Cold acclimation increases mitochondrial oxidative capacity without inducing mitochondrial uncoupling in goldfish white skeletal muscle. *Biol. Open* **2**, 82-87.

Fangue, N. A., Hofmeister, M. and Schulte, P. M. (2006). Intraspecific variation in thermal tolerance and heat shock protein gene expression in common killifish, *Fundulus heteroclitus*. *J. Exp. Biol.* **209**, 2859-2872.

Fangue, N. A., Richards, J. G. and Schulte, P. M. (2009). Do mitochondrial properties explain intraspecific variation in thermal tolerance? *J. Exp. Biol.* **212**, 514-522.

Fry, F. E. J. and Hart, J. S. (1948). The relation of temperature to oxygen consumption in the goldfish. *Biol. Bull.* **94**, 66-77.

Gnaiger, E., Lassnig, B., Kuznetsov, A., Rieger, G. and Margreiter, R. (1998). Mitochondrial oxygen affinity, respiratory flux control and excess capacity of cytochrome *c* oxidase. *J. Exp. Biol.* **201**, 1129-1139.

Grim, J. M., Miles, D. R. B. and Crockett, E. L. (2010). Temperature acclimation alters oxidative capacities and composition of membrane lipids without influencing activities of enzymatic antioxidants or susceptibility to lipid peroxidation in fish muscle. *J. Exp. Biol.* **213**, 445-452.

Guderley, H. (2004). Metabolic responses to low temperature in fish muscle. *Biol. Rev.* **79**, 409-427.

Guderley, H. (2011). Mitochondria and temperature. In *Encyclopedia of Fish Physiology* (ed. A. P. Farrell), pp. 1709-1716. Amsterdam: Elsevier Inc.

Hagve, T.-A., Woldseth, B., Brox, J., Narce, M. and Poisson, J.-P. (2009). Membrane fluidity and fatty acid metabolism in kidney cells from rats fed purified eicosapentaenoic acid or purified docosahexaenoic acid. *Scand. J. Clin. Lab. Invest.* **58**, 187-194.

Hazel, J. R. (1984). Effects of temperature on the structure and metabolism of cell membranes in fish. *Am. J. Physiol.* **246**, R460-R470.

Hazel, J. R. (1995). Thermal adaptation in biological membranes: is homeoviscous adaptation the explanation? *Annu. Rev. Physiol.* **57**, 19-42.

Hazel, J. R. and Landrey, S. R. (1988). Time course of thermal adaptation in plasma membranes of trout kidney. II. Molecular species composition. *Am. J. Physiol.* **255**, R628-R634.

Healy, T. M. and Schulte, P. M. (2012). Thermal acclimation is not necessary to maintain a wide thermal breadth of aerobic scope in the common killifish (*Fundulus heteroclitus*). *Physiol. Biochem. Zool.* **85**, 107-119.

Iles, A. C. (2014). Towards predicting community-level effects of climate: relative temperature scaling of metabolic and ingestion rates. *Ecology* **95**, 2657-2668.

Itoi, S., Kinoshita, S., Kikuchi, K. and Watabe, S. (2003). Changes of carp F_oF_1-ATPase in association with temperature acclimation. *Am. J. Physiol. Regul. Integr. Comp. Physiol.* **284**, R153-R163.

Khan, J. R., Iftikar, F. I., Herbert, N. A., Gnaiger, E. and Hickey, A. J. R. (2014). Thermal plasticity of skeletal muscle mitochondrial activity and whole animal respiration in a common intertidal triplefin fish, *Forsterygion lapillum* (Family: Tripterygiidae). *J. Comp. Physiol. B* **184**, 991-1001.

Kraffe, E., Marty, Y. and Guderley, H. (2007). Changes in mitochondrial oxidative capacities during thermal acclimation of rainbow trout *Oncorhynchus mykiss*: roles of membrane proteins, phospholipids and their fatty acid compositions. *J. Exp. Biol.* **210**, 149-165.

Lemoine, N. P. and Burkepile, D. E. (2012). Temperature-induced mismatches between consumption and metabolism reduce consumer fitness. *Ecology* **93**, 2483-2489.

Leray, C., Chapelle, S., Duportail, G. and Florentz, A. (1984). Changes in fluidity and 22:6(n−3) content in phospholipids of trout intestinal brush-border membrane as related to environmental salinity. *Biochim. Biophys. Acta* **778**, 233-238.

Li, Z., Agellon, L. B., Allen, T. M., Umeda, M., Jewell, L., Mason, A. and Vance, D. E. (2006). The ratio of phosphatidylcholine to phosphatidylethanolamine influences membrane integrity and steatohepatitis. *Cell Metab.* **3**, 321-331.

Liu, X., Strable, M. S. and Ntambi, J. M. (2011). Stearoyl CoA desaturase 1: role in cellular inflammation and stress. *Adv. Nutr.* **2**, 15-22.

Marsh, D. (2010). Structural and thermodynamic determinants of chain-melting transition temperatures for phospholipid and glycolipids membranes. *Biochim. Biophys. Acta* **1798**, 40-51.

McBryan, T. L., Healy, T. M., Haakons, K. L. and Schulte, P. M. (2016). Warm acclimation improves hypoxia tolerance in *Fundulus heteroclitus*. *J. Exp. Biol.* **219**, 474-484.

McKenzie, J. L., Dhillon, R. S. and Schulte, P. M. (2016). Steep, coincident, and concordant clines in mitochondrial and nuclear-encoded genes in a hybrid zone between subspecies of Atlantic killifish, *Fundulus heteroclitus*. *Ecol. Evol.* **6**, 5771-5787.

Mulligan, C. M., Le, C. H., deMooy, A. B., Nelson, C. B. and Chicco, A. J. (2014). Inhibition of delta-6 desaturase reverses cardiolipin remodeling and prevents contractile dysfunction in the aged mouse heart without altering mitochondrial respiratory function. *J. Gerontol. A Biol. Sci. Med. Sci.* **69**, 799-809.

Muriana, F. J. G., Vazquez, C. M. and Ruiz-Gutierrez, V. (1992). Fatty acid composition and properties of the liver microsomal membrane of rats fed diets enriched with cholesterol. *J. Biochem.* **112**, 562-567.

Paradies, G., Paradies, V., De Benedictis, V., Ruggiero, F. M. and Petrosillo, G. (2014). Functional role of cardiolipin in mitochondrial bioenergetics. *Biochim. Biophys. Acta* **1837**, 408-417.

Paton, C. M. and Ntambi, J. M. (2009). Biochemical and physiological function of stearoyl-CoA desaturase. *Am. J. Physiol. Endocrinol. Metab.* **297**, E28-E37.

Pörtner, H. (2001). Climate change and temperature-dependent biogeography: oxygen limitation of thermal tolerance in animals. *Naturwissenschaften* **88**, 137-146.

Salin, K., Auer, S. K., Anderson, G. J., Selman, C. and Metcalfe, N. B. (2016). Inadequate food intake at high temperatures is related to depressed mitochondrial respiratory capacity. *J. Exp. Biol.* **219**, 1356-1362.

Santigosa, E. and Vagner, M. (2011). Characterization and modulation of gene expression and enzymatic activity of delta-6 desaturase in teleosts: a review. *Aquaculture* **315**, 131.

Schlame, M. (2007). Assays of cardiolipin levels. In *Mitochondria*, 2nd edn (ed. L. A. Pon and E. A. Schon), pp. 223-240. Amsterdam: Elsevier.

Schlame, M. (2013). Cardiolipin remodeling and the function of tafazzin. *Biochim. Biophys. Acta* **1831**, 582-588.

Sinensky, M. (1974). Homeoviscous Adaptation—a homeostatic process that regulates the viscosity of membrane lipids in *Escherichia coli*. *Proc. Natl. Acad. Sci. USA* **71**, 522-525.

Sparagna, G. C., Johnson, C. A., McCune, S. A., Moore, R. L. and Murphy, R. C. (2005). Quantitation of cardiolipin molecular species in spontaneously hypertensive heart failure rats using electrospray ionization mass spectrometry. *J. Lipid Res.* **46**, 1196-1204.

St-Pierre, J., Charest, P. M. and Guderley, H. (1998). Relative contribution of quantitative and qualitative changes in mitochondria to metabolic compensation during seasonal acclimatisation of rainbow trout *Oncorhynchus mykiss*. *J. Exp. Biol.* **201**, 2961-2970.

Stillwell, W. and Wassall, S. R. (2003). Docosahexaenoic acid: membrane properties of a unique fatty acid. *Chem. Phys. Lipids* **126**, 1-27.

Strobel, A., Graeve, M., Pörtner, H. O. and Mark, F. C. (2013). Mitochondrial acclimation capacities to ocean warming and acidification are limited in the Antarctic Nototheniid fish, *Notothenia rossii* and *Lepidonotothen squamifrons*. *PLoS ONE* **8**, e68865.

Sunday, J. M., Bates, A. E. and Dulvy, N. K. (2011). Global analysis of thermal tolerance and latitude in ectotherms. *Proc. R. Soc. B Biol. Sci.* **278**, 1823-1830.

Tasseva, G., Bai, H. D., Davidescu, M., Haromy, A., Michelakis, E. and Vance, J. E. (2013). Phosphatidylethanolamine deficiency in Mammalian mitochondria impairs oxidative phosphorylation and alters mitochondrial morphology. *J. Biol. Chem.* **288**, 4158-4173.

Taylor, W. A., Dolinsky, V. W., Hatch, G. M. and Ma, B. J. (1999). Acylation of monolysocardiolipin in rat heart. *J. Lipid Res.* **40**, 1837-1845.

Tosi, F., Sartori, F., Guarini, P., Olivieri, O. and Martinelli, N. (2014). Delta-5 and Delta-6 desaturases: crucial enzymes in polyunsaturated fatty acid-related pathways with pleiotropic influences in health and disease. In *Oxygen Transport to Tissue XXXI* (ed. E. Takahashi and D. F. Bruley), pp. 61-81. Cham: Springer International Publishing.

van den Thillart, G. and Modderkolk, J. (1978). The effect of acclimation temperature on the activation energies of state III respiration and on the unsaturation of membrane lipids of goldfish mitochondria. *Biochim. Biophys. Acta* **510**, 38-51.

van der Veen, J. N., Lingrell, S., da Silva, R. P., Jacobs, R. L. and Vance, D. E. (2014). The concentration of phosphatidylethanolamine in mitochondria can modulate ATP production and glucose metabolism in mice. *Diabetes* **63**, 2620-2630.

Vance, D. E., Li, Z. and Jacobs, R. L. (2007). Hepatic phosphatidylethanolamine N-methyltransferase, unexpected roles in animal biochemistry and physiology. *J. Biol. Chem.* **282**, 33237-33241.

Virtue, S., Dale, M., Tan, C. Y., Bidault, G., Hagen, R., Griffin, J. L. and Vidal-Puig, A. (2015). Brown adipose tissue thermogenic capacity is regulated by Elovl6. *Cell Rep.* **13**, 2039-2047.

Wodtke, E. (1981). Temperature adaptation of biological membranes. The effects of acclimation temperature on the unsaturation of the main neutral and charged phospholipids in mitochondrial membranes of the carp (*Cyprinus carpio* L.). *Biochim. Biophys. Acta* **640**, 698-709.

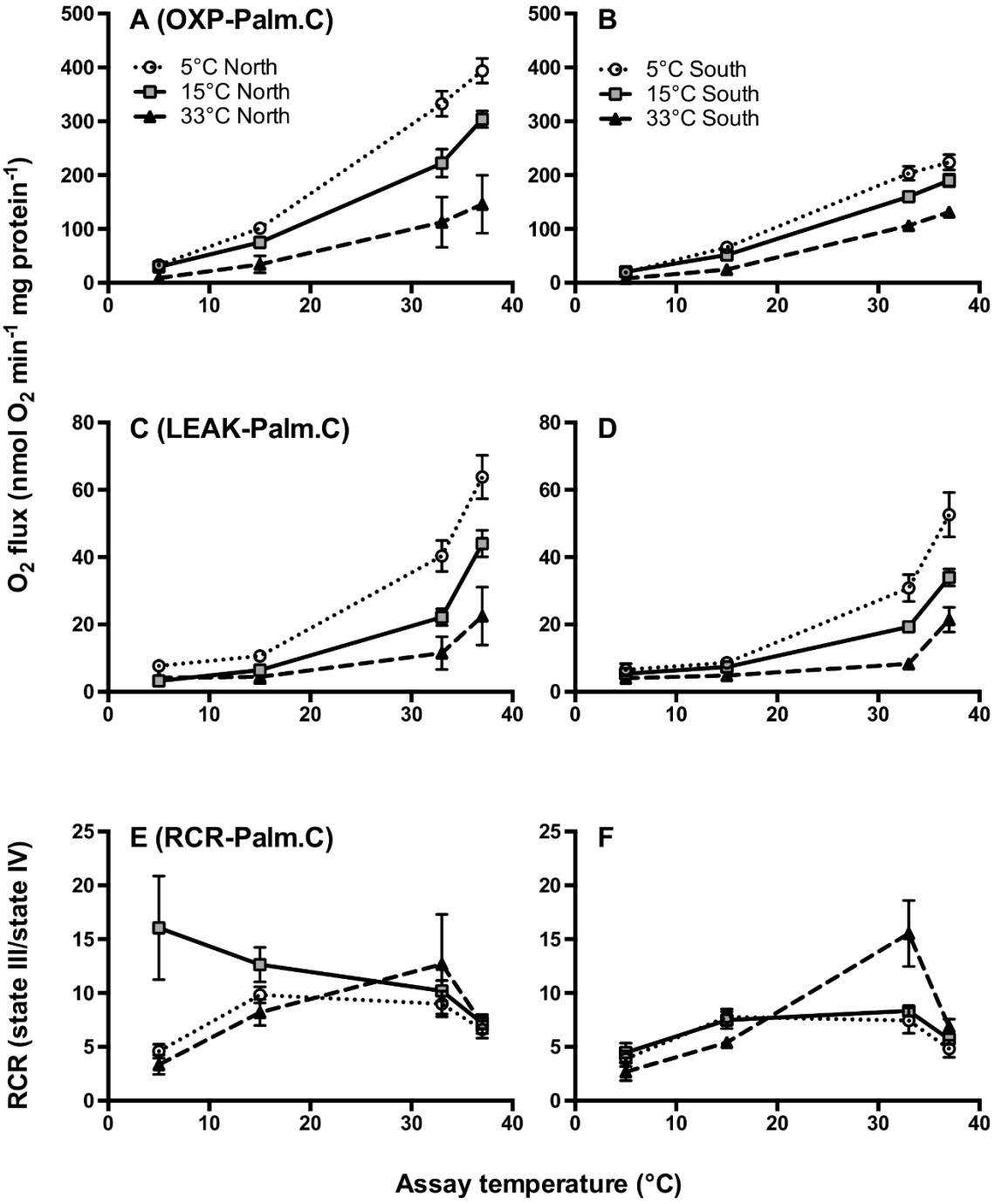

Figure S1. *Fundulus heteroclitus* coupled liver mitochondrial respiration and respiratory control ratio fuelled with fatty-acid substrates. Northern (A, C, E) and southern (B, D, F) *F. heteroclitus* were acclimated to 5, 15 or 33°C for four weeks. Oxidative phosphorylation (OXP, state 3; A, B) and LEAK (state 2; C, D) respiration rate were measured with fatty-acid substrates (palmitoyl carnitine and malate). Respiratory control ratio (E, F) was calculated as the ratio of OXP/LEAK. Data are mean ± SEM; see Table 1 for associated statistics (n = 7-8).

Journal of Experimental Biology • Supplementary information

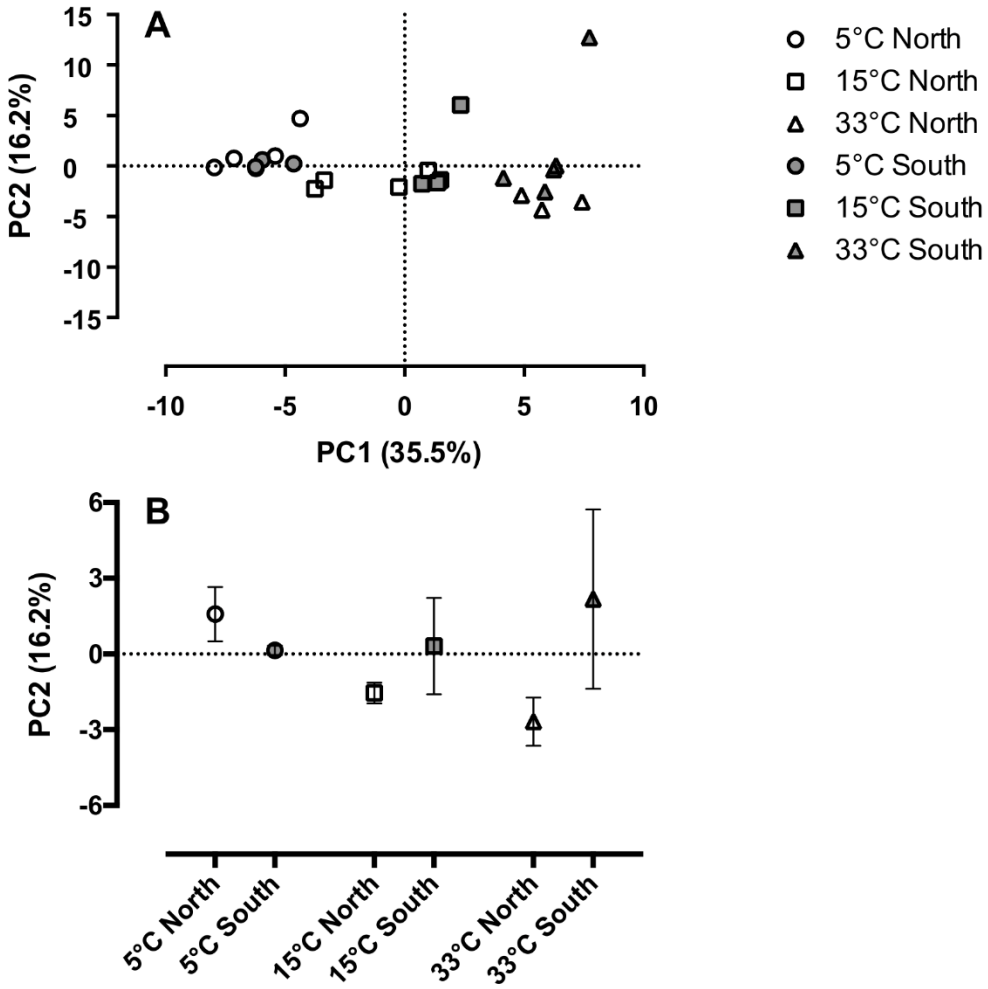

Figure S2. Second principal component score for liver mitochondrial membrane composition of thermally acclimated *Fundulus heteroclitus* subspecies. Northern (white symbols) and southern (grey symbols) were acclimated to 5, 15, or 33°C for four weeks. (A) the plot of individuals along PC1 and PC2 axes. PC2 did not significantly separate subspecies of thermal acclimation treatment (B). See the Results section for associated statistics, $n = 4$.

Journal of Experimental Biology • Supplementary information

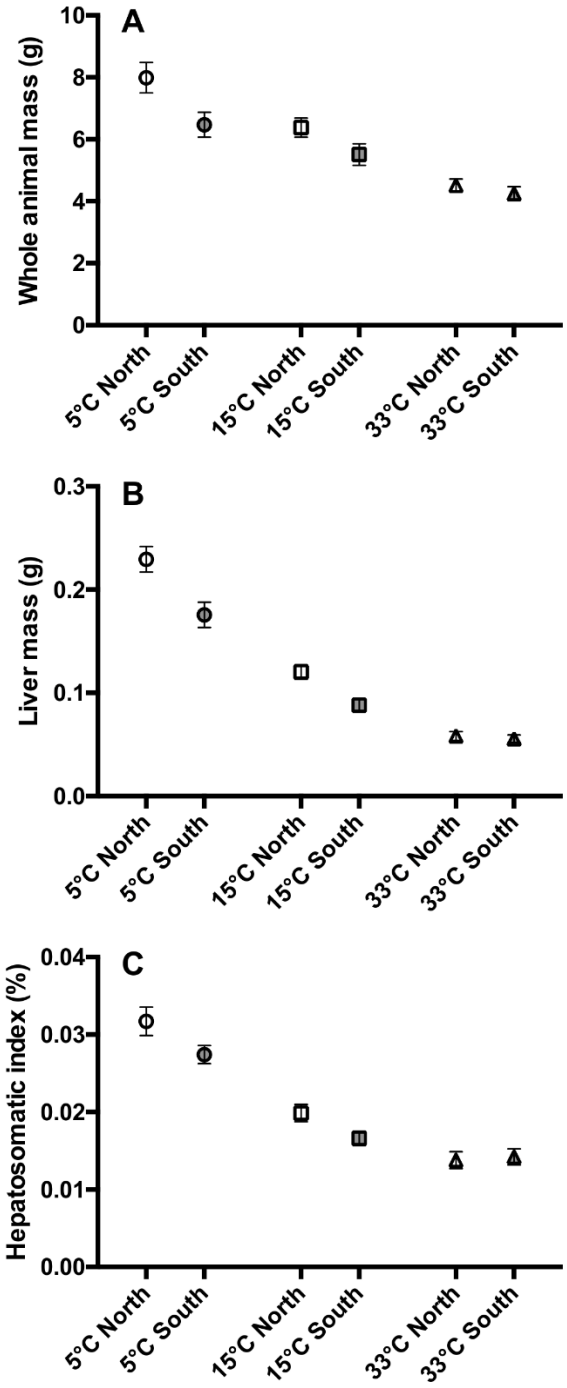

Figure S3. *Fundulus heteroclitus* whole-animal, liver wet mass, and somatic index. Northern and southern *F. heteroclitus* were acclimated to 5, 15, or 33°C for four weeks. Hepatosomatic index (C) was calculated as the ratio of wet liver mass to whole-animal mass. Data are mean ± SEM; see Results for associated statistics (n = 49-56).

Journal of Experimental Biology • Supplementary information

Supplemental Table 1. Principal component analysis factor scores, percent contribution (Ctr) of individual variables to the components, and the squared cosines of the variables on principal components 1 and 3.

	F_1	F_3	Ctr_1	Ctr_3	Cos_1^2	Cos_3^2
CL	0.42	-0.24	0.67	0.80	17.6	5.6
Monolyso-CL	0.83	-0.16	**2.63**	0.39	69.5	2.7
PE	0.59	-0.56	**1.33**	**4.49**	35.1	31.7
PC	-0.35	0.75	0.45	**7.88**	12.0	55.6
CL_1402	0.74	0.29	**2.09**	1.20	55.1	8.5
CL_1404	0.91	0.10	**3.11**	0.15	82.0	1.0
CL_1424	-0.76	0.26	**2.17**	0.98	57.2	6.9
CL_1428	0.85	-0.04	**2.76**	0.02	73.0	0.2
CL_1448	-0.77	0.20	**2.26**	0.54	59.8	3.8
CL_1450	0.59	-0.04	**1.33**	0.02	35.1	0.2
CL_1452	0.75	-0.16	**2.14**	0.38	56.5	2.7
CL_1472	-0.75	0.37	**2.13**	**1.94**	56.2	13.7
CL_1476	0.81	0.36	**2.49**	**1.83**	65.6	12.9
CL_1496	-0.89	0.03	**2.98**	0.01	78.5	0.1
CL_1498	0.06	-0.85	0.02	**10.13**	0.4	71.4
CL_1500	0.88	0.19	**2.92**	0.49	77.2	3.4
CL_1520	0.66	-0.05	**1.66**	0.04	43.8	0.3
CL_1522	0.88	0.29	**2.96**	1.19	78.2	8.4
CL_1544	-0.72	-0.26	**1.95**	0.94	51.5	6.7
CL_1546	0.72	0.00	**1.94**	0.00	51.1	0.0
CL_1566	-0.74	0.08	**2.10**	0.10	55.3	0.7
CL_1568	-0.04	0.32	0.01	**1.44**	0.2	10.2
MLCL_1164	-0.22	0.59	0.19	**4.87**	5.0	34.4
MLCL_1166	-0.36	0.34	0.49	**1.64**	13.1	11.5
MLCL_1186	-0.81	0.07	**2.50**	0.07	66.0	0.5
MLCL_1188	-0.01	-0.15	0.00	0.30	0.0	2.1
MLCL_1190	0.05	0.19	0.01	0.49	0.3	3.5
MLCL_1210	0.29	0.42	0.32	**2.51**	8.4	17.7
MLCL_1212	0.47	0.49	0.85	**3.38**	22.4	23.8
MLCL_1234	-0.50	-0.52	0.95	**3.78**	25.1	26.7
MLCL_1236	0.90	-0.18	**3.04**	0.44	80.2	3.1
MLCL_1256	-0.23	0.10	0.19	0.15	5.1	1.0
MLCL_1258	0.71	0.29	**1.89**	1.23	49.9	8.7
MLCL_1282	-0.10	-0.42	0.04	**2.53**	0.9	17.8
PC_14:0	-0.08	0.21	0.02	0.65	0.7	4.6
PC_16:0	0.46	0.28	0.80	1.12	21.2	7.9
PC_16:1	0.80	-0.19	**2.40**	0.49	63.4	3.5
PC_18:0	-0.70	0.36	**1.85**	**1.86**	48.8	13.1
PC_18:1n9	0.25	0.04	0.24	0.03	6.3	0.2
PC_18:1n7	0.83	0.15	**2.63**	0.33	69.4	2.3

Journal of Experimental Biology • Supplementary information

Supplemental Table 1. Principal component analysis factor scores, percent contribution (Ctr) of individual variables to the components, and the squared cosines of the variables on principal components 1 and 3.

	F_1	F_3	Ctr_1	Ctr_3	Cos_1^2	Cos_3^2
PC_18:2n6	0.09	-0.58	0.03	**4.76**	0.8	33.6
PC_18:3n6	-0.24	-0.08	0.21	0.08	5.6	0.6
PC_18:3n3	-0.26	-0.10	0.25	0.15	6.5	1.1
PC_20:0	-0.37	-0.11	0.51	0.16	13.5	1.1
PC_20:1	-0.14	-0.09	0.08	0.11	2.0	0.8
PC_20:2	-0.31	-0.16	0.36	0.35	9.5	2.5
PC_20:4n6	0.25	-0.16	0.25	0.37	6.5	2.6
PC_20:3n6	-0.51	0.00	1.00	0.00	26.4	0.0
PC_20:3n3	-0.48	-0.25	0.89	0.86	23.5	6.1
PC_20:5n3	0.22	-0.34	0.19	1.67	4.9	11.8
PC_22:0	-0.60	0.08	**1.36**	0.10	35.9	0.7
PC_22:1	-0.46	-0.07	0.82	0.07	21.5	0.5
PC_22:4	-0.31	-0.40	0.36	**2.31**	9.6	16.3
PC_22:5n3	-0.40	0.05	0.60	0.03	15.8	0.2
PC_22:6n3	0.72	0.07	**1.96**	0.08	51.7	0.5
PE_14:0	-0.81	0.06	**2.47**	0.05	65.2	0.3
PE_16:0	-0.75	-0.03	**2.13**	0.02	56.2	0.1
PE_16:1	-0.25	0.56	0.23	**4.47**	6.1	31.5
PE_18:0	-0.53	0.12	1.07	0.21	28.2	1.5
PE_18:1n9	0.73	0.34	**2.04**	**1.68**	53.8	11.9
PE_18:1n7	0.18	-0.42	0.12	**2.46**	3.1	17.4
PE_18:2n6	0.60	-0.49	**1.34**	**3.43**	35.5	24.2
PE_18:3n6	-0.35	0.31	0.46	**1.38**	12.2	9.7
PE_18:3n3	0.58	0.18	1.29	0.44	34.1	3.1
PE_20:0	0.19	-0.25	0.13	0.88	3.5	6.2
PE_20:1	0.73	0.16	**2.00**	0.35	52.8	2.5
PE_20:2	0.67	0.45	**1.71**	**2.82**	45.2	19.9
PE_20:4n6	-0.70	-0.26	**1.84**	0.99	48.5	7.0
PE_20:3n6	0.84	0.36	**2.69**	**1.84**	70.9	12.9
PE_20:3n3	-0.39	0.47	0.57	**3.16**	15.2	22.3
PE_20:5n3	0.69	0.11	**1.81**	0.17	47.8	1.2
PE_22:0	-0.82	0.21	**2.53**	0.65	66.7	4.6
PE_22:1	-0.42	-0.29	0.68	**1.16**	18.0	8.2
PE_22:4	0.72	-0.04	**1.98**	0.02	52.1	0.2
PE_22:5n3	-0.71	-0.10	**1.91**	0.14	50.3	1.0
PE_22:6n3	0.65	-0.35	**1.61**	**1.75**	42.5	12.4

The important contributions (Ctr) are in bold, indicating a greater than average variable contribution to the respective principal component (i.e., Ctr > $\frac{1}{76}$ or 1.31%). CL: cardiolipin; MLCL: monolysocardiolipin; PC: phosphatidylcholine; PE: phosphatidylethanolamine. Squared cosines have been multiplied by 100 for ease of interpretation. $n = 4$

Journal of Experimental Biology • Supplementary information

Supplemental Table 2. Hepatic mitochondrial phospholipid class distribution and cardiolipin molecular species from thermally acclimated *Fundulus heteroclitus* subspecies.

Mitochondrial PL classes	5°C		15°C		33°C	
	North	South	North	South	North	South
CL	27.8±1.15	24.3±2.02	24.7±.93	21.3±.60	22.0±.77	22.4±2.11
MLCL (*†‡)	3.2±.28	1.7±.26	1.6±.12	9.7±.05	7.4±.09	7.2±.02
PE (†‡)	31.0±.83	24.6±1.21	30.0±1.47	30.6±.33	33.2±.99	28.2±1.39
PC (*‡)	41.1±.89	51.0±.90	45.1±1.92	48.0±.75	44.7±.68	49.3±1.08
PC/PE (*‡)	1.3±.04	2.1±.07	1.5±.14	1.6±.04	1.4±.05	1.8±.08
CL Molecular species						
CL_1402 (*)	0.9±.11	1.1±.11	0.5±.06	0.9±.19	0.1±.05	0.05±.01
CL_1404 (*)	$1.6±1.1x10^{-3}$	$1.4±6.7x10^{-4}$	$0.7±9.2x10^{-4}$	$0.9±2.2x10^{-3}$	$0.01±2.3x10^{-5}$	$0.03±1.3x10^{-4}$
CL_1424 (*‡)	0.6±.05	0.9±.04	0.9±.12	1.6±.16	1.7±.13	1.4±.20
CL_1428 (*)	3.3±.17	2.2±.19	1.7±.22	2.2±.39	0.2±.05	0.2±.03
CL_1448 (*)	2.4±.04	4.0±.11	4.0±.46	6.5±.35	9.6±1.08	7.7±1.93
CL_1450 (*)	5.6±.31	6.3±.33	6.3±.34	6.2±.62	3.7±.58	3.7±.82
CL_1452 (*)	4.4±.24	3.6±.19	4.2±.55	4.2±.26	1.7±.33	1.7±.24
CL_1472 (*‡)	5.7±.38	6.6±.55	6.0±.38	9.3±1.05	9.9±.24	8.7±.27
CL_1476 (*†)	6.6±.76	8.9±.25	4.0±.24	5.3±.21	2.3±.28	2.6±.32
CL_1496 (*)	6.7±.50	7.7±.36	11.8±1.47	13.9±1.12	23.2±.94	18.3±2.37
CL_1498 (*‡)	10.9±.23	7.9±.34	14.4±.56	9.6±.97	8.2±.95	11.7±.79
CL_1500 (*)	7.8±.33	9.1±.52	6.4±.27	6.7±.53	3.2±.35	3.8±.65
CL_1520 (*)	8.2±.28	7.0±.25	6.9±.21	6.7±.71	5.4±.58	5.4±.69
CL_1522 (*†)	4.8±.21	6.4±.08	2.5±.21	2.7±.24	1.0±.41	1.5±.32
CL_1544 (*)	11.8±.72	6.8±.58	15.9±.96	9.5±.84	21.9±2.06	24.4±3.97
CL_1546 (*)	6.6±.49	6.4±.25	5.3±.35	3.8±.96	3.5±.47	4.3±1.05
CL_1566 (*)	1.0±.14	0.68±.11	1.0±.14	1.0±.13	2.6±.37	2.2±.44
CL_1568	0.7±.11	1.1±.13	0.6±.10	0.7±.12	0.8±.32	1.0±.16
MLCL_1164 (*)	4.4±.53	6.1±.52	3.4±.27	8.3±.57	5.6±.95	5.8±.95
MLCL_1166	2.8±.39	4.1±.33	2.3±.69	3.5±.45	4.2±.29	4.0±1.20
MLCL_1186 (*)	5.4±.37	8.9±.30	9.6±1.54	13.4±.14	17.4±2.78	16.0±.17
MLCL_1188 (*)	7.9±.46	8.4±.88	11.9±.97	10.7±.27	9.5±1.21	6.8±1.95
MLCL_1190	6.0±.42	7.0±.47	5.4±.71	6.4±1.51	5.8±.56	6.1±1.86
MLCL_1210	10.5±1.05	11.4±.62	8.2±.49	10.2±.53	8.8±1.36	9.7±.85
MLCL_1212 (*)	7.6±.77	9.3±.84	3.8±.66	5.7±1.15	5.4±.81	5.5±.90
MLCL_1234 (*)	14.2±.78	12.2±1.54	20.9±.99	13.5±1.17	19.8±2.83	20.8±2.79
MLCL_1236 (*†)	17.0±1.06	13.7±1.38	14.7±2.08	9.5±.77	5.7±.69	5.2±.73
MLCL_1256	4.8±1.19	3.9±.33	4.9±.85	6.2±1.33	5.7±1.00	5.2±1.45
MLCL_1258 (*)	8.0±.48	6.9±.65	3.3±1.15	5.1±1.12	2.8±1.73	1.4±.20
MLCL_1282	10.8±1.65	7.5±.75	10.8±1.33	7.0±.83	8.6±1.12	13.0±2.94

Data are mean % of total head group or fatty acid ± SEM (n = 4). Symbols indicate significant effects from a two-way ANOVA *: acclimation; †: subspecies; ‡: acclimation x subspecies. The number following CL or MLCL corresponds to the MW of the PL species and corresponds to the FA chains as indicated below. CL: cardiolipin; MLCL: monolysocardiolipin; PC: phosphatidylcholine; PE: phosphatidylethanolamine. PC\PE: the ratio of phosphatidylcholine to phosphatidylethanolamine.

Journal of Experimental Biology • Supplementary information

Supplemental Table 3. Fatty acid composition of cardiolipin and monolysocardiolipin molecular species determined by HPLC-ESI-MS/MS

CL Molecular Species (m/z)	16:0	16:1	18:1	18:2	18:3	20:4	22:6
CL_1402	1	1	2				
CL_1404	2		2				
CL_1424		1	1	2			
CL_1428		1	3				
CL_1448				4			
CL_1450			1	3			
CL_1452			2	2			
CL_1472				3		1	
CL_1476			2	1		1	
CL_1496				3			1
CL_1498			1	2			1
CL_1500			2	1			1
CL_1520				2		1	1
CL_1522			1	1		1	1
CL_1544				2			2
CL_1546			1	1			2
CL_1566					1	1	2
CL_1568				1		1	2
MLCL_1164		1	2				
MLCL_1166	1		2				
MLCL_1186				3			
MLCL_1188			1	2			
MLCL_1190			2	1			
MLCL_1210				2		1	
MLCL_1212			1	1		1	
MLCL_1234				1		2	
MLCL_1236			1			2	
MLCL_1256					1	1	1
MLCL_1258				1		1	1
MLCL_1282				1			2

CL: Cardiolipin, MLCL: monolysocardiolipin, m/z: mass to charge ratio (equivalent to molecular weight). The number following CL or MLCL corresponds to the MW of the PL species and corresponds to the FA chains.

Journal of Experimental Biology • Supplementary information

Supplemental Table 4. Total hepatic mitochondrial phospholipid FA composition from thermally acclimated *Fundulus heteroclitus* subspecies.

	5°C acclimated		15°C acclimated		33°C acclimated	
Fatty acids	North	South	North	South	North	South
14:0 (*)	0.9±.06	1.0±.05	1.0±.06	1.0±.03	1.2±.06	1.0±.06
16:0 (*)	16.7±.32	17.2±.17	17.4±.31	17.2±.34	18.3±.37	17.5±.36
16:1 (*†)	2.1±.09	1.9±.13	1.8±.09	1.4±.14	1.1±.001	0.9±.02
18:0 (*†)	9.3±.24	10.7±.09	9.8±.11	12.5±.26	13.1±.44	13.6±.58
18:1n9	12.7±.37	13.8±.19	12.8±.43	11.5±.35	12.6±.61	13.4±.75
18:1n7 (*†)	4.4±.18	3.7±.07	3.4±.11	2.4±.06	1.5±.05	1.1±.14
18:2n6 (*†)	6.8±.23	5.6±.09	7.6±.34	6.4±.19	6.6±.30	6.3±.40
18:3n6 (*)	0.21±.031	0.27±.027	0.34±.015	0.19±.037	0.18±.036	0.17±.052
18:3n3 (*)	$0.19\pm1.4\times10^{-4}$	$0.15\pm1.0\times10^{-4}$	$0.18\pm7.1\times10^{-5}$	$0.17\pm 9.1\times10^{-5}$	$0.20\pm4.5\times10^{-5}$	$0.21\pm1.5\times10^{-4}$
20:0 (*†)	0.48±.068	0.29±.014	0.39±.036	0.28±.028	0.31±.025	0.24±.041
20:1 (*)	1.3±.07	1.2±.06	1.0±.04	0.8±.04	0.6±.06	0.7±.08
20:2 (*)	1.0±.11	1.0±.07	0.9±.06	0.7±.03	0.6±.03	0.8±.12
20:4n6 (*)	6.8±.23	7.2±.24	5.8±.27	6.2±.13	5.3±.20	5.7±.28
20:3n6 (*)	0.40±.053	0.50±.040	0.35±.062	0.34±.022	0.47±.037	0.57±.105
20:3n3 (*)	0.69±.086	0.59±.041	0.72±.065	0.68±.039	0.92±.055	0.97±.149
20:5n3 (‡)	2.6±.16	1.8±.14	1.7±.12	2.0±.11	1.3±.08	1.9±.23
22:0 (*)	0.9±.07	0.8±.06	1.1±.07	1.1±.06	1.4±.12	1.4±.16
22:1 (*)	0.61±.088	0.43±.021	0.62±.046	0.57±.025	0.68±.059	0.78±.097
22:4	1.8±.09	1.6±.09	1.2±.24	1.4±.05	1.4±.20	2.1±.26
22:5n3 (*†)	9.2±.21	8.1±.38	10.3±.23	10.4±.50	12.7±.89	10.7±.64
22:6n3 (*)	20.0±.37	21.6±.46	20.2±.60	21.2±.49	18.2±.68	17.5±.82

Fatty acid data are mean % of total ± SEM (n = 7-8). Symbols indicate significant effects from a two-way ANOVA *: acclimation; †: subspecies; ‡: acclimation x subspecies.

Journal of Experimental Biology • Supplementary information

Supplemental Table 5. Hepatic mitochondrial phosphatidylcholine (PC) fatty composition from thermally acclimated *Fundulus heteroclitus* subspecies.

	5°C		15°C		33°C	
Phosphatidylcholine (PC) fatty acids	North	South	North	South	North	South
PC_14:0	0.7±.14	0.6±.03	0.5±.16	0.7±.04	0.5±.12	0.6±.10
PC_16:0	19.7±1.99	20.4±.61	18.0±.84	17.9±1.23	18.6±.73	15.9±2.18
PC_16:1 (*)	1.8±.09	1.5±.07	1.5±.18	1.3±.14	0.7±.04	1.0±.16
PC_18:0 (†)	7.6±.77	7.5±.41	7.3±.86	10.1±.27	11.3±.64	10.1±1.26
PC_18:1n9	12.2±.41	13.2±.34	12.8±.86	11.1±.73	13.0±.74	11.3±2.51
PC_18:1n7 (*)	2.7±.20	2.9±.06	1.9±.27	1.5±.15	1.0±.06	1.5±.48
PC_18:2n6	5.7±.52	4.7±.07	6.2±.82	5.3±.31	4.9±.38	5.5±.43
PC_18:3n6	0.8±.66	0.2±.03	0.1±.04	0.8±.55	0.1±.05	1.4±.69
PC_18:3n3	0.9±.83	0.1±.003	0.1±.05	0.9±.75	0.1±.04	1.8±.93
PC_20:0	0.8±.44	0.2±.01	0.3±.15	1.3±1.12	0.3±.03	2.8±1.45
PC_20:1	1.2±.49	1.0±.07	0.7±.08	1.0±.52	0.4±.09	1.9±.63
PC_20:2	1.2±.67	0.6±.08	0.8±.24	1.1±.66	0.5±.03	2.5±1.02
PC_20:4n6	3.8±.20	3.6±.25	3.3±.32	3.6±.21	2.2±.64	3.8±.66
PC_20:3n6	0.9±.35	0.5±.02	0.7±.27	0.9±.38	1.1±.29	1.7±.58
PC_20:3n3	0.5±.20	0.2±.01	0.3±.14	0.5±.17	0.5±.22	1.2±.42
PC_20:5n3	2.1±.19	1.6±.11	2.0±.26	1.9±.28	0.9±.11	2.0±.51
PC_22:0 (*)	1.2±.19	0.8±.08	1.1±.39	1.3±.17	1.7±.30	2.1±.65
PC_22:1	0.7±.11	0.4±.05	0.6±.24	0.5±.10	0.8±.19	1.7±.83
PC_22:4	0.3±.06	0.4±.21	1.3±.51	0.8±.12	1.1±.32	0.6±.27
PC_22:5n3	11.2±1.64	9.8±0.91	12.2±3.01	11.1±1.50	18.0±1.98	11.0±0.81
PC_22:6n3 (*)	18.3±2.24	25.0±1.00	20.6±3.31	18.0±2.13	14.8±0.96	11.6±2.07

Data are mean % of total head group or fatty acid ± SEM (n = 4). Symbols indicate significant effects from a two-way ANOVA *: acclimation; †: subspecies; ‡: acclimation x subspecies.

Journal of Experimental Biology • Supplementary information

Supplemental Table 6. Hepatic mitochondrial phosphatidylethanolamine (PE) fatty composition from thermally acclimated *Fundulus heteroclitus* subspecies.

	5°C		15°C		33°C	
Phosphatidylethanolamine (PE) fatty acids	North	South	North	South	North	South
PE_14:0 (*)	0.9± .08	0.8±.11	1.1±.11	1.6±.16	1.5±.13	1.5±.03
PE_16:0 (*)	12.7±.43	11.6±.68	13.1±.75	14.5±.35	14.9±.31	14.5±.19
PE_16:1	0.7±.10	0.6±.05	0.3±.13	0.8±.18	1.2±.41	0.6±.16
PE_18:0 (*†)	13.1±.46	15.3±0.39	13.7±1.23	16.0±0.91	15.4±0.48	17.6±0.65
PE_18:1n9 (*)	6.9±.15	6.6±.36	3.1±1.08	2.7±.14	3.3±.18	3.1±.30
PE_18:1n7	4.4±.41	3.9±.13	4.3±.63	4.3±.18	3.7±.22	4.2±.25
PE_18:2n6 (*)	2.0±.21	1.6±.11	2.2±.45	1.2±.27	1.0±.13	0.8±.05
PE_18:3n6	0.2±.04	0.1±.05	0.1±.05	0.3±.05	0.3±.02	0.3±.11
PE_18:3n3 (*)	0.4±.04	0.3±.04	0.2±.08	0.3±.06	0.2±.02	0.1±.06
PE_20:0	0.4±.01	0.3±.04	0.5±.29	0.3±.06	0.3±.07	0.1±.09
PE_20:1 (*)	1.3±.11	1.3±.10	0.7±.27	1.1±.45	0.2±.14	0.1±.10
PE_20:2 (*)	0.8±.06	1.0±.07	0.4±.16	0.4±.16	0.5±.19	0.06±.06
PE_20:4n6 (*)	0.4±.03	0.3±.03	3.4±1.08	4.7±.68	3.9±.41	3.6±.06
PE_20:3n6 (*)	6.4±.24	7.7±.44	2.1±1.21	1.4±.15	1.4±.30	0.6±.38
PE_20:3n3 (*)	1.1±.08	1.1±.06	0.4±.29	0.7±.33	1.6±.33	1.7±.27
PE_20:5n3 (*)	2.3±.26	2.3±.10	1.8±.24	1.5±.25	1.4±.37	1.2±.22
PE_22:0 (*)	1.6±.09	1.6±.16	2.0±.10	2.5±.27	2.9±.31	2.6±.19
PE_22:1 (*)	0.6±.02	0.6±.02	1.4±.41	1.0±.12	1.1±.14	0.9±.11
PE_22:4 (*)	3.2±.74	3.1±.73	2.2±1.53	1.2±.91	1.1±.46	1.6±.39
PE_22:5n3 (*)	15.2±.40	16.1±0.72	21.7±1.96	22.3±2.47	22.4±1.23	21.2±0.65
PE_22:6n3 (*)	16.7±1.54	15.8±2.51	16.2±4.38	9.2±5.43	9.9±4.08	11.5±1.35

Data are mean % of total head group or fatty acid ± SEM (n = 4). Symbols indicate significant effects from a two-way ANOVA *: acclimation; †: subspecies; ‡: acclimation x subspecies.

Journal of Experimental Biology • Supplementary information

Supplemental Table 7. Characteristics of hepatic mitochondrial phospholipid fatty acid composition from thermally acclimated *Fundulus heteroclitus* subspecies.

	5°C acclimated		15°C acclimated		33°C acclimated	
Total Phospholipids	North	South	North	South	North	South
MUFA/PUFA (*‡)	0.43±.013	0.43±.010	0.42±.019	0.36±.011	0.37±.021	0.41±.062
DBI (*)	2.5±.028	2.5±.019	2.5±.037	2.5±.019	2.4±.056	2.3±.062
n3/n6 (*‡)	2.3±.048	2.4±.069	2.4±.035	2.6±.047	2.7±.119	2.5±.117
Total n3 PUFA	0.328±.0043	0.323±.0043	0.332±.0064	0.347±.0037	0.334±.0105	0.314±.0111
Total n6 PUFA (*†‡)	0.143±.0020	0.135±.0028	0.141±.0017	0.132±.0011	0.126±.0021	0.127±.0017
Total n7 PUFA (*†‡)	0.078±.0018	0.068±.0015	0.062±.0017	0.045±.0017	0.031±.0008	0.027±.0008
Chain length	19.18±.037	19.15±.022	19.19±.035	19.27±.035	19.19±.063	19.24±.079
Phosphatidylcholine	North	South	North	South	North	South
PC-MUFA/PUFA	0.4±.02	0.4±.01	0.3±.01	0.4±.09	0.3±.02	0.4±.04
PC-DBI	2.4±.09	2.6±.05	2.5±.07	2.2±.25	2.4±.10	2.1±.04
PC-n3/n6 (‡)	3.1±.48	4.0±.19	3.4±.29	2.7±.49	4.1±.38	2.3±.33
PC-Total n3 PUFA	0.3±.02	0.3±.01	0.3±.01	0.3±.04	0.3±.01	0.2±.01
PC-Total n6 PUFA (‡)	0.11±.015	0.09±.003	0.10±.006	0.11±.014	0.09±.005	0.13±.017
PC-Total n7 PUFA (*‡)	0.06±.007	0.05±.001	0.04±.004	0.04±.007	0.02±.001	0.04±.005
PC-Chain length	19.0±.05	19.2±.05	19.3±.06	19.3±.14	19.2±.10	19.1±.11
Phosphatidylethanolamine	North	South	North	South	North	South
PE-MUFA/PUFA (*)	0.31±.009	0.27±.008	0.20±.012	0.24±.032	0.22±.019	0.23±.004
PE-DBI(*‡)	2.7±.03	2.7±.07	2.8±.14	2.4±.06	2.4±.08	2.4±.01
PE-n3/n6 (*‡)	3.9±.19	3.6±.19	5.1±.55	4.4±.45	5.5±.64	6.6±.44
PE-Total n3 PUFA (‡)	0.38±.003	0.38±.011	0.43±.021	0.38±.002	0.39±.013	0.40±.003
PE-Total n6 PUFA (*)	0.09±.004	0.10±.004	0.08±.004	0.08±.007	0.07±.007	0.06±.003
PE-Total n7 PUFA	0.06±.005	0.06±.002	0.05±.009	0.07±.008	0.05±.002	0.05±.002
PE-Chain length (‡)	19.6±.06	19.6±.06	19.7±.12	19.4±.04	19.4±.04	19.5±.03

Symbols indicate significant effects from a two-way ANOVA *: acclimation; †: subspecies; ‡: acclimation x subspecies. MUFA/PUFA: the ratio of monounsaturated fatty-acid to polyunsaturated fatty-acid. DBI: fatty acid double-bound (unsaturation) index. n3/n6: the ratio of n3 PUFA to n6 PUFA. n = 7-8 (total PL) or 4 (PE and PC).

Journal of Experimental Biology • Supplementary information

Supplemental Table 8. Hepatic mitochondrial phospholipid fatty acid product/precursor ratios and their associated desaturase and elongase enzymes.

			5°C		15°C		33°C	
Product	**Precursor**	**Enzyme**	North	South	North	South	North	South
18:0	16:0	Elovl6 (*†‡)	0.55±.020	0.62±.009	0.56±.011	0.72±.021	0.71±.028	0.78±.033
18:1n7	16:1n7	Elovl6 (*)	2.1±.12	2.0±.12	1.8±.05	1.7±.16	1.4±.05	1.2±.14
20:0	18:0	Elovl6 (*†)	0.05±.018	0.03±.003	0.04±.009	0.02±.005	0.02±.004	0.02±.008
20:1n9	18:1n9	Elovl6 (*)	0.10±.008	0.08±.005	0.07±.005	0.06±.002	0.04±.002	0.05±.004
22:0	20:0	Elovl6	0.02±.014	0.04±.020	0.01±.009	0.03±.015	0.01±.008	0.01±.009
22:1n9	20:1n9	Elovl6 (*)	0.45±.051	0.36±.025	0.62±.030	0.76±.071	1.28±.191	1.22±.204
20:2n6	18:2n6	Elovl5 (*)	0.15±.020	0.18±.013	0.11±.011	0.11±.005	0.10±.004	0.13±.023
20:3n3	18:3n3	Elovl5	3.72±.650	3.86±.232	3.86±.398	4.01±.471	4.56±.290	4.60±.526
20:3n6	18:3n6	Elovl5 (*)	2.19±.534	1.89±.167	1.03±.196	2.07±.315	3.31±.793	2.98±.632
22:4n6	20:4n6	Elovl4/5 (*)	0.26±.007	0.23±.014	0.22±.041	0.23±.010	0.26±.028	0.36±.037
22:5n3	20:5n3	Elovl4/5 (*†‡)	3.54±.260	4.74±.588	5.94±.388	5.18±.451	9.54±.555	6.13±.758
18:1n9	18:0	SCD (*†‡)	1.38±.044	1.29±.023	1.30±.042	0.92±.034	0.96±.024	0.97±.031
16:1n7	16:0	SCD (*†)	0.12±.003	0.10±.006	0.10±.005	0.08±.008	0.05±.002	0.05±.001
18:3n6	18:2n6	Δ6D (‡)	0.03±.003	0.04±.004	0.04±.002	0.03±.005	0.02±.004	0.02±.010
22:6n3	22:5n3	Δ6D[#] (*†)	2.17±.074	2.69±.150	1.97±.090	2.07±.141	1.47±.133	1.66±.137
20:4n6	20:3n6	Δ5D (*)	18.9±2.24	14.7±1.08	19.1±2.16	18.5±1.72	11.6±1.11	11.5±1.70
20:4n6	18:2n6	Δ6D/Elovl5/Δ5D (*†)	1.02±.072	1.28±.055	0.79±.071	0.97±.053	0.81±.068	0.94±.109
20:3n6	20:2n6	Δ8D (*†)	0.38±.035	0.49±.021	0.40±.049	0.48±.027	0.71±.032	0.68±.041

Data are mean ± SEM (n = 7-8). Symbols indicate significant effects from a two-way ANOVA. *: acclimation; †: subspecies; ‡: acclimation x subspecies. [#]: Reaction also requires Elovl2/4/5 and peroxisomal β-oxidation; or can be catalyzed by Δ4D. Elovl, elongase; Δ6D, Δ-6 desaturase; Δ5D, Δ-5 desaturase; Δ8D, Δ-8 desaturase; SCD, stearoyl-CoA desaturase.

Journal of Experimental Biology • Supplementary information